Received: 4 October 2024 | Revised: 20 February 2025 | Accepted: 21 February 2025

DOI: 10.1002/alz.70101

Alzheimer's & Dementia®
THE JOURNAL OF THE ALZHEIMER'S ASSOCIATION

RESEARCH ARTICLE

Targeting of phosphorylated tau at threonine 181 by a Qβ virus-like particle vaccine is safe, highly immunogenic, and reduces disease severity in mice and rhesus macaques

Nicole M. Maphis[1] | **Jonathan Hulse**[2] | **Julianne Peabody**[2] | **Somayeh Dadras**[2] | **Madelin J Whelpley**[2] | **Manas Kandath**[2] | **Colin Wilson**[3] | **Sasha Hobson**[4] | **Jeff Thompson**[4] | **Suttinee Poolsup**[2] | **Danielle Beckman**[5] | **Sean P Ott**[5] | **Jennifer W. Watanabe**[5] | **Jodie L. Usachenko**[5] | **Koen K Van Rompay**[5] | **John Morrison**[5] | **Reed Selwyn**[3] | **Gary Rosenberg**[4] | **Janice Knoefel**[4] | **Bryce Chackerian**[2] | **Kiran Bhaskar**[2]

[1]Department of Neuroscience, 1 University of New Mexico, Albuquerque, New Mexico, USA

[2]Department of Molecular Genetics and Microbiology, 1 University of New Mexico, Albuquerque, New Mexico, USA

[3]Department of Radiology, 1 University of New Mexico, Albuquerque, New Mexico, USA

[4]Center for Memory and Aging, 1 University of New Mexico, Albuquerque, New Mexico, USA

[5]California National Primate Research Center, University of California, Davis, California, USA

Correspondence
Kiran Bhaskar, Ph.D., MSC08 4660, 1 University of New Mexico, Albuquerque, NM 87131, USA.
Email: kbhaskar@salud.unm.edu

Funding information
New Mexico Higher Education Department – Technology Enhancement Fund (TEF); University of New Mexico (UNM) Health Sciences Center Bridge Support; UNM Department of Molecular Genetics and Microbiology intradepartmental grant; National Institute on Aging - MarkVCID-II, Grant/Award Number: U24AG21886; New Mexico Alzheimer's Disease Research Center (NM ADRC), Grant/Award Number: P30AG086404-01; CNPRC Pilot Program, Grant/Award Number: P51OD011107; National Institutes of Health to the California National Primate Research Center; UNM Center for Biomedical Research Excellence (CoBRE); Center for Brain Recovery and Repair Pre-Clinical Core, Grant/Award Number: P20GM109089; Autophagy, Inflammation, and

Abstract

INTRODUCTION: Pathological accumulation of tau (pTau) contributes to various tauopathies, including Alzheimer's disease (AD), and correlates with cognitive decline. A rapid surge in tau-targeted approaches via anti-sense oligonucleotides, active/passive immunotherapies suggests that targeting p-Tau is a viable strategy against tauopathies.

METHOD: We describe a multi-species validation of our previously described Qß virus-like particle (VLP)–based vaccine technology targeting phosphorylated tau on threonine 181 (pT181-Qß).

RESULTS: Two vaccine doses of pT181-Qß, without any adjuvants, elicited robust antibody responses in two different mouse models of tauopathy (PS19 and hTau) and rhesus macaques. In mouse models, vaccination reduced AT180+ hyperphosphorylated, Sarkosyl insoluble, Gallyas silver positive tau, inflammasomes/neuroinflammation, and improved recognition memory and motor function without inducing adverse T-cell activation. Anti-pT181 antibodies are reactive to pTau in human AD brains, engage pT181+ tau in human brain lysates, and are central nervous system bioavailable.

Nicole Maphis and Jonathan Hulse contributed equally to this work.

Metabolism (AIM) CoBRE Center, Grant/Award Number: P20GM121176-04; Institutional Research and Academic Career Development Award, Grant/Award Number: IRACDA # NIH K12GM088021; NIH Research Evaluation and Commercialization Hubs (REACH) Loan Repayment Program; National Centralized Repository for Alzheimer's Disease and Related Dementias (NCRAD), Grant/Award Number: U24AG21886; National Institute of General Medical Sciences, Grant/Award Numbers: K12GM088021, IRACDA; NIH Office of the Director, Grant/Award Number: P51OD011107; National Institute of Neurological Disorders and Stroke, Grant/Award Numbers: RF1NS083704-05A1, R01NS083704

DISCUSSION: Our results suggest the translational utility of pT181-Qß against tauopathies.

KEYWORDS
Alzheimer's disease, hTau, immunotherapy, mild cognitive impairment, non-human primates, PS19, pT181, rhesus macaques, tau, tauopathies, vaccines, virus-like particles

Highlights

- Icosahedral display of phosphorylated tau at threonine 181 (pT181) Qß virus-like particle surface ("pT181-Qß" vaccine) induces a robust immune response in mice and in non-human primates (NHPs)
- pT181-Qß vaccination reduces pathological tau (pTau) and brain atrophy, and improves memory and motor function in PS19 and hTau mice.
- pT181-Qß vaccination–induced immunoglobulin Gs (IgGs) are safe, Th2 skewed (anti-inflammatory), specific to pTau in human AD brain, and efficiently engage pT181 in NHPs and human brain lysate.
- $pT181^{+}$ tau in human plasma correlates with the neurofilament light in subjects with mild cognitive impairment (MCI)—suggesting the presence of pT181-Qß vaccine target in the early disease state.

1 | BACKGROUND

Tauopathies are a group of neurodegenerative diseases where microtubule-associated protein tau (MAPT) undergoes hyperphosphorylation and aggregates as soluble oligomers, paired-helical filaments (PHFs), or mature neurofibrillary tangles (NFTs) in different brain regions. Recent advances in electron and atomic force microscopy have demonstrated significant heterogeneity in PHFs and NFTs, linked to a spectrum of clinical presentations in different tauopathies. Notably, tau phosphorylated (p) at threonine (T) residues, such as 181, 205, 217, and 231, appear early in disease progression.[1–4] Elevated levels of pT181 and pT217 serve as established fluid biomarkers for diagnosing Alzheimer's disease (AD) and other tauopathies.[4–7] Due to pTau's connection to tauopathies and its direct link to clinical symptoms, numerous trials have been conducted to decrease pTau burden.

Based on the recent U.S. Food and Drug Administration (FDA) approvals of amyloid beta (Aβ)–targeted monoclonal antibody (mAb) immunotherapies (lecanemab and donanemab), there is renewed interest in immunotherapy against pTau. Preclinical studies using passive immunotherapy with mAbs have provided critical proof-of-principle data supporting pTau as a therapeutic target. However, passive tau immunotherapies that completed preclinical testing (e.g., AbbVie's ABBV-8E12) have failed futility analyses in Phase 2 clinical trials.[8] Several possible reasons for these failures include the region of tau targeted, dosing, and route of administration. More broadly, mAb therapies are expensive, require long-term repeated infusions, and often elicit immune responses, thereby limiting their effectiveness. Some trials have shown limited efficacy for reducing tau burden but have varying effects on clinical outcomes, such as slowing cognitive decline. Despite the reasonably safe profile, central nervous system (CNS) bioavailability, target engagement, and decent half-life exhibited by these strategies, the major limitation of current tau immunotherapies is their requirement for repeated infusions.

Active vaccination against tau is an alternative approach with the theoretical potential to elicit more durable anti-tau antibody responses. However, thus far, vaccine efforts have been marked by weak and transient antibody responses. At least two active immunotherapies, AADvac1 (Axon Neuroscience) and ACI-35 (AC Immune/Janssen), are in clinical development. AADvac1 consists of tau amino acid (aa) 294-305, linked to a keyhole limpet hemocyanin (KLH) carrier protein. Although this vaccine can elicit anti-tau antibodies, it requires six doses and elicits weak and short-lived antibody responses.[9] ACI-35 consists of a liposome-displayed phosphorylated tau peptide (aa 393-408) adjuvanted with monophosphoryl lipid A (MPLA). However, immunogenicity data from preclinical studies suggest that ACI-35 is also poorly immunogenic,[10] and patients in the clinical trial received multiple injections of high doses of vaccine (as much as 1800 µg) (presented at the Tau 2024 Global Conference). The poor immunogenicity of tau vaccines may result from immune tolerance and the vaccine platform utilized.

We previously developed a vaccine (pT181-Qß) in which a pT181 peptide is displayed at high valency on the surface of a virus-like particle (VLP) derived from the Qß bacteriophage.[11] pT181-Qß elicited high-titer and long-lasting antibody responses against tau, which is consistent with other data indicating that multivalent display on VLPs is an efficient method for eliciting strong antibody responses

RESEARCH IN CONTEXT

1. **Systematic review**: A literature review of PubMed and other literature sources suggests that the pathological modifications in tau protein strongly correlate with the cognitive decline in Alzheimer's disease (AD) and related dementias. As such, many pre-clinical and clinical trials have been targeting pathological tau to determine if such an approach benefits patients. Emerging clinical trials using monoclonal antibodies (mAbs) against different regions of tau show positive results in secondary outcomes of cognitive stabilization. Even if the mAb is approved for tau, repeated infusions of mAbs may have compliance issues in elderly patients and short-lived antibody responses upon active immunizations. The relevant citations and clinical trials are included where appropriate.
2. **Interpretation**: Our study suggests that display of phosphorylated tau (on T181) peptide on the virus-like particles (VLPs) from Qβ bacteriophage induced a robust immune response, reduced tau pathology, prevented brain atrophy, and improved memory, and that the immunoglobulin Gs (IgGs) from immunized sera engaged the target in vaccinated non-human primates (rhesus macaques) and human AD brains.
3. **Future directions**: Targeting pT181-positive tau with pT181-Qβ vaccination may in Phase 0/1 clinical trials validate the safety, immunogenicity, and therapeutic efficacy of pT181-Qβ vaccination in patients with AD and related tauopathies.

against self-antigens.[12,13] We chose to target pT181 for the following reasons: (1) it is a well-established cerebrospinal fluid (CSF) biomarker for AD and other tauopathies[14]; (2) it is secreted into the extracellular space by neurons,[15,16] providing ample opportunity for antibody binding; (3) it is present in the mid-region of tau, which does not undergo pre-shedding (unlike N- or C-terminal targets[17,18]) prior to secretion; and (4) plasma pT181 levels are more strongly correlated with AD severity than total tau levels.[19] Vaccination with pT181-Qß successfully reduced tau pathology and cognitive decline in the rTg4510 mouse model, which carries a *P301L* tau mutation.[11] Furthermore, pT181-Qß vaccination reduced inflammasome markers in vaccinated rTg4510 mice.[20] Here, we expanded these studies to evaluate the immunogenicity and efficacy of pT181-Qß in two additional mouse models of tauopathy (PS19 and hTau) and adult rhesus macaques. We show that immunization with pT181-Qß is well tolerated, and that vaccination elicits strong, durable, and efficacious anti-tau antibody responses. It is important to note that anti-tau antibodies cross-react with pT181 in human AD brain lysates.

2 | METHODS

2.1 | Ethical statement—mice

The University of New Mexico (UNM) Institutional Animal Care and Use Committee (IACUC) approved all animal procedures described in the study (IACUC protocol #s: 19-200841-B-HSC (Breeding); 18-200761-HSC (Experimental)). All mice were housed in a specific pathogen-free (SPF) facility within the Animal Research Facility (ARF) at UNM, in a 12 h light/dark cycle with ad libitum access to food (Envigo's 2920 diet) and water. Mice were housed in 85 in^2 ventilated micro isolator cages supplemented with sterilized and autoclaved TEK-Fresh standard crinkle bedding; environmental enrichment included tissue paper, wooden twigs, and an elevated penthouse insert. Mice used in this study were not used for breeding and were housed by sex at a density of two to five mice per cage. All animals chosen for experimental manipulation were healthy, of average weight, and had no history of any medical conditions, including rectal prolapse, skin dermatitis, or malocclusion.

2.2 | Mice (PS19)

The P301S mouse model (PS19 line)[21] overexpresses the *P301S* mutation in human MAPT, *Mapt*, driven under the mouse prion promoter (PrP) and was purchased from Jackson laboratories (Stock #008169). This transgenic line was backcrossed into the C57Bl/6j mouse model from Jackson laboratories (B6, stock #000664) and maintained in this inbred strain for more than five generations before use.

2.3 | Mice (hTau)

The hTau mice (also known as hTau$^{MaptKO(Duke)}$[22]) were generated by crossing the line 8c[23,24] (from Drs. Peter Davis and Karen Duff) with $Mapt^{+/+}$ to complete mouse tau knockout mice $MaptKO^{Duke}$[25] (generous gift from Drs. Hanna Dawson and Michael Vitek). hTau mice were maintained in the C57Bl/6j background.

2.4 | Conjugation of pT181 peptide to Qß VLPs and vaccination design in PS19, hTau, and rhesus macaques

As described previously,[11] a 13-amino acid tau peptide phosphorylated at threonine 181 (^{175}TPPAPK**pT**PPSSGE^{187}:GGC; referred to as pT181) was modified with a two-glycine and one-cysteine spacer sequence (underlined residues) for conjugation via the bifunctional cross-linker succinimidyl 6-[(beta-maleimidopropionamido) hexanoate] (SMPH; Thermo Fisher Scientific, catalog #22363) to the surface-exposed lysines on the Qß-VLPs, which were produced in *Escherichia coli* as described previously.[26,27] pT181 peptide was conjugated to surface-exposed lysines on Qß-VLPs. The Qß-VLP molecular model was drawn with Jmol: an open-source Java viewer for chemical structures in three dimensions, http://www.jmol.org/. Efficiency of

conjugation was confirmed via gel electrophoresis on a 10% Sodium Dodecyl Sulfate (SDS) denaturing polyacrylamide gel.

2.5 | Vaccination of PS19 and hTau mice with pT181-Qß or Qß-VLPs

The first injection (prime) (either the pT181-Qß or the control [Qß—platform alone]), was administered intramuscularly (i.m.) to 3-month-old P301S (PS19) mice. Four weeks following the first injection, mice were assessed for anti-pT181 titer in the sera before being administered their second injection (boost) at 4 months of age. At ≈8.5 months, vaccinated and control-immunized P301S mice were subjected to cognitive assessments through the Novel Object Recognition (NOR) task, for gait impairments using the Catwalk (PS19) and Y-maze (hTau). Following behavioral assessment, these mice were imaged using a 7.0 Tesla (T) magnetic resonance imaging (MRI) for T2-weighted imaging. A final antibody titer was re-evaluated after the experiment's conclusion (≈9 months of age). After the experiment, mice were sacrificed for biochemical and neuropathological assessments.

For hTau mice, the first injection (prime) (pT181-Qß or the control Qß [platform alone]) was administered (i.m.) to 6-month-old hTau mice. The second shot (boost) was given 4 weeks after the first dose. Four weeks following the first injection, mice were assessed for anti-pT181 titer in the sera. At ≈11.5 months of age, the vaccinated and control-immunized hTau mice were subjected to cognitive (working memory) assessments through the Y-maze task. A final antibody titer was re-evaluated after the experiment's conclusion (≈12 months of age), and then the animals were sacrificed for biochemical and neuropathological assessments.

2.6 | Peripheral hematological analysis in pT181-Qβ or Qβ vaccinated PS19 mice

A cohort of mice—n = 5 nTg littermates, n = 10 Qβ, n = 12 pT181-Qβ P301S—were assessed at 6 months of age (2 months following boost and 3 months following prime injection) for complete blood count (CBC) using the VetScan HM5 (Zoetis, USA). The VetScan HM5 Hematology Analyzer is a five-part differential hematology analyzer used in veterinary offices and animal research facilities. Briefly, 50 µL of blood (via retro-orbital sinus) was collected through ethylenediaminetetraacetic acid (EDTA)–coated glass pipettes in mice under isoflurane gas anesthesia (induction at 4% isoflurane, maintenance at 1.5%–2%, within a mix of 2:1 O_2:NO_2 gas). Data obtained from the VetScan software was Z-scored and normalized (MATLAB). These values were plotted using the Complex Heat Map Function within the Bioconductor package in R Studio.

2.7 | Elispot dual-color interleukin (IL)-4/interferon (IFN)-γ T-cell stimulation assay

The 2-month-old C57Bl/6j mice were immunized with either unconjugated Qß-VLPs or conjugated pT181-Qß-VLPs (n = 8 per group) as described previously using a two-dose series spaced 2 weeks apart. An age-matched group of unvaccinated C57Bl/6j mice was used as a negative control (n = 3). One week or 5 weeks after the second injection, the animals were sacrificed by cardiac blood collection. Spleens were collected on ice in Hank's balanced salt solution (Sigma-Aldrich; cat no: H6648). Splenocytes were collected by flushing the spleens with 3 mL of Roswell Park Memorial Institute (RPMI) 1640 media with L-glutamine (Cytiva; cat no. SH30027), then crushing the tissue through a 100 µM cell filter and rinsing with 1 mL of RPMI media. The cells were pelleted by centrifugation at 400 × g for 5 min at 4°C and resuspended in Cellular Technology Limited (C.T.L) media supplemented with L-glutamine. The cells were counted using a Countess II cell counter (Thermo Fisher Scientific) and diluted to an appropriate concentration for plating.

The ImmunoSpot System T-cell double-color enzymatic mouse IFN-γ/IL-4 Elispot assay (C.T.L; cat #mIFNgIL4-1 M/2) was performed according to the manufacturer's instructions. Briefly, the plates were coated with IL-4 and IFN-γ capture antibody overnight prior to the experiment. Antigen solutions for T-cell stimulation were prepared by diluting either unconjugated Qß-VLPs or unconjugated pT181 tau peptides at 6 µg/100 µL per well in C.T.L media. A vehicle group using an equivalent amount of phosphate-buffered saline (PBS) in C.T.L media was used to determine background levels of activated T cells. The splenocytes were plated at 100,000 cells/well and incubated at 37°C with 5% CO_2 for 24 h. The plates were then washed, and the enzymatic ImmunoSpot reaction was performed to visualize IL-4 and IFN-γ secreting T-cell spots. The dried plates were then imaged and quantified by C.T.L using their kit scanning services, and statistical analysis was performed using two-way analysis of variance (ANOVA).

2.8 | Assessment of humoral response in PS19 and hTau mice

To characterize the peripheral anti-pT181 titer, blood was collected via retro-orbital capillary collection at 4 and ≈8.5 months of age (for PS19) or 7 and 12 months of age (for hTau) and analyzed via enzyme-linked immunosorbent assay (ELISA) using the 16-mer tau peptide (pT181) as the antigen. Briefly, immulon-2 plates were incubated with 500 ng streptavidin (Thermo Fisher Scientific, catalog #434301) in pH 7.4 PBS overnight at 4°C. Following washing, SMPH was added to the wells at 1 µg/well and incubated for 2 h at room temperature (RT). pT181 peptide was added to the wells at 1 µg/well and incubated overnight at 4°C. The plate was subsequently blocked with 0.5% milk in PBS for 2 h. Four-fold dilutions of sera were added to each well and incubated for 2.5 h. The wells were probed with horseradish peroxidase (HRP)–conjugated secondary antibody—goat anti-mouse-IgG (Jackson ImmunoResearch, catalog #115-005-003; 1:4000) for 1 h. The reaction was developed using 3,3′, 5,5′-tetramethylbenzidine (TMB) substrate (Thermo Fisher Scientific, catalog # 34028) and stopped using 1% HCl. The reactivity of sera for the target antigen was determined by measuring optical density at 450 nm (OD_{450}). Wells with twice the OD_{450} of the background were positive, and the highest dilution value with a positive value was considered the end-point dilution titer.

2.9 | NOR (PS19 and hTau mice)

On the first day of this two-day paradigm, animals were acclimated to an open 75 cm^2 arena for 5 min. Twenty-four hours later, the mice were exposed to two identical objects (two Lego Towers) for 5 min. Following a 1 h interval, the mice were exposed to one of the previous familiar objects (Lego Tower) and a novel object (a short, wide, plastic jar of beige sand). A greater percentage of time spent with the novel object versus time spent with the familiar object was identified as intact delay-dependent memory. Results were acquired with Ethovision XT8 (Noldus) and then processed in Excel and Prism.

2.10 | Y-maze (hTau mice)

Mice were allowed to freely explore a Y-maze for 1 min, and the number of arm entries, sequence of arm entries, and number of repeated arm entries were recorded using the Ethovision Noldus and then processed in Excel and Prism.

2.11 | Morris water maze (PS19 mice)

The Morris water maze (MWM) test involved a 6-day paradigm which included an acquisition phase (5 days) and a probe trial (1 day). During the acquisition phase, animals freely navigated the tank, full of cold water (25 degrees C +/− 2 degrees) with powdered milk to obfuscate the hidden platform. Over 5 days (4 trials, with a 25 minute inter-trial interval) animals were trained to navigate to a hidden platform using spatial cues on the wall. During the acquisition phase, the animals freely navigated the tank for up to 1 min and were able to successfully navigate to the hidden platform within 20 seconds by the fifth day. On the sixth day, a probe trial was performed by removing the platform and the percentage of time spent in the target quadrant versus the other quadrants; this was recorded as a measurement of working spatial memory. All data were recorded using the Ethovision Noldus and then processed in Excel and Prism.

2.12 | Catwalk (PS19 mice)

Gait analysis was performed using the Catwalk XT system (Noldus). Animals were allowed to walk freely across a glass runway to reach a goal box containing an empty cage. A compliant run trial was defined as a mouse moving across the runway without stopping or changing directions with a consistent speed within a time frame of 1–10 s. Note: Typical run durations are 0.5–5 s, but the interval was extended to accommodate these differences due to the overweight and slow nature of these mice at 9 months of age. Two to three compliant runs were averaged for one trial per mouse. A high-speed camera recorded the paw contacts from below, and data were exported into Excel and analyzed in Prism.

2.13 | MRI and Image processing (PS19)

Animals were imaged using a 7.0 T Biospec MRI scanner (Bruker Biospin; Billerica) equipped with a single-tuned surface coil for the mouse brain. Briefly, mice were anesthetized with isoflurane gas (induction dose 2%–3%; maintenance dose 1.5%–2%) with a mixture of O_2:NO_2 gases in a ratio of 2:1, delivered during the recording period (≈1 h). T2-weighted (T2w) images were used to assess gray matter regional volumetrics and quantified across six separate regions of interest (ROIs—cortical [aqua-cyan], hippocampal [dark blue], ventricle [green], striatum [pink], corpus callosum [light brown], and cerebellar [light blue]) drawn using the freehand draw tool in VivoQuant version 3.0.1 (inviCRO, LLC, Boston, MA) with the Allen Brain Atlas reference (www.allenbrainatlas.org). Four representative coronal slices are presented. The ROI was hand-drawn around the six ROIs on every MR brain slice ($n = 24$ slices per mouse were pre-processed in Paravision version 5.1, Bruker, Germany). Image contrast thresholding and ROI-based volumetric analysis were performed using VivoQuant.

2.14 | Detergent soluble protein extraction, gel electrophoresis, and Western blot

Hippocampal brain tissues (from PS19 and hTau mice) were first homogenized for 1 min in 10 volumes of Tissue Protein Extraction Reagent/mg of tissue (TPER, Thermo Scientific, catalog #78510) with phosphatase and protease inhibitor cocktails (Sigma Aldrich, P5726 and P8340, respectively), and then sonicated for 30 s at 30% amplitude on ice before being centrifuged at 12,000 × *g* for 30 min at 4°C. Samples were prepared using the soluble lysates from the centrifugation and 1x lithium dodecyl sulfate/reducing agent (LDS/RA—Thermo Fisher Scientific) following the manufacturer's instructions. Insoluble hippocampal pellets (P1) were frozen at −80°C until they could be processed for Sarkosyl insoluble extraction (*described below*). Hippocampal soluble samples made up in LDS/RA were boiled at 95 for 15 min prior to being resolved on a NuPage 4%–12% Bis-Tris Gel (Thermo Fisher Scientific) with 2-(N-morpholino)ethanesulfonic acid (MES) running buffer and immunoblotted overnight in transfer buffer. All blots were processed in parallel and derived from the same experiment. The dilutions of primary antibodies were as follows: AT8 (Thermo Fisher Scientific, MN1020) 1:10,000, AT180 (Thermo Fisher Scientific MN1040) 1:5000, PHF1 (a kind gift from the late Peter Davies) 1:10,000, Tau5 (MAB-361), Tau12 (MAB2241), GAPDH (AB2302) (Millipore, 1:20,000), ASC (AL177, Adipogen AG-25B-006-C100) 1:1000, NLRP3 (MAB—Adipogen AG-20B-0014-C100), and Caspase-1 (Rabbit polyclonal SantaCruz Biotech sc-514).

2.15 | Sarkosyl-insoluble/soluble protein analysis

The Sarkosyl-insoluble isolation of tau was isolated from hippocampal tissues as described previously.[11,28] Briefly, TPER soluble hippocampal

tissue was processed as indicated above. Protein levels for all samples were estimated using Bicinchoninic acid (BCA) assay (Thermofisher Scientific Cat#23225) and equal protein levels (3.5 mg) were aliquoted for Sarkosyl isolation. We sonicated the detergent-insoluble pellet (P1) with 10 volumes of cold Buffer H (10 mM Tris-HCl, 1 mM ethylene glycol-bis(2-aminoethyl ether)-N,N,N',N'-tetraacetic acid (EGTA), 0.8 mM Sodium Chloride (NaCl) 10% sucrose, pH 7.4) supplemented by 0.1 mM phenylmethanesulfonyl fluoride (PMSF) (Sigma-Aldrich). After centrifugation at 34,000 × *g* in a Beckman Ti TLA-120.2 rotor for 30 min at 4°C, the supernatant (S1) was adjusted to 1% w/v with N-laurylsarcosine (Sigma-Aldrich) and 1% (v/v) 2-mercaptoethanol and incubated at 37°C for 2 h with agitation. After centrifugation at 600,000 x *g* for 35 min at RT, the Sarkosyl-soluble supernatant (S2) was aspirated and resuspended in 1x LDS/RA sample buffer. The Sarkosyl-insoluble pellet (P2) was washed several times in 1% Sarkosyl solution and prepared in buffer H. Equal protein levels across samples were loaded onto a NuPAGE 4%–12% Bis-Tris Gel (Thermo Fisher Scientific), and western blotting was performed as described earlier.

2.16 | Immunohistochemistry (IHC)

Following sacrifice, hemi-brains were post-fixed in 4% paraformaldehyde/0.125 M phosphate buffer (PFA/PB) for a period of 24 h before cryoprotection using cryoprotection solution containing sucrose and glycerol (300 g/L: 300 mL/Lin Sorenson's buffer) for at least 24 h before sectioning. Hemi-brains were sectioned 30 µm thick on a Leica sliding knife freezing/sliding microtome and placed into a cryo-storage solution (0.2 M PO_4 500 mL/L; polyvinylpyrrolidone [PVP 40] 10 g/L; sucrose 300 g/L, and ethylene glycol 300 mL/L– pH 7.4). Sagittal brain tissue sections were stored at −20°C until immunohistochemistry staining. Briefly, free-floating sagittal brain tissue sections were washed with PBS, antigen retrieval was performed by boiling in 0.1 M sodium citrate/PBS, and tissues were washed 3 times × 5 min in 1x PBS. Next, endogenous peroxidase was blocked with 3% H_2O_2/PBS, and tissues were rewashed with PBS containing 0.1% Triton (PBST) before blocking with 5% normal goat serum (NGS) in 0.4% PBST for 1 h. Primary antibodies (AT8, AT180, 1:500; Iba1, 1:500, and anti-pT181 sera 1:100) were diluted in 5% NGS/0.4% PBST and incubated overnight at 4°C. The next day, sections were washed with PBST and incubated in secondary antibodies (biotinylated goat anti-mouse or biotinylated goat anti-rabbit, 1:250) in 5% NGS/0.4% PBST for 1 h at RT, then with Avidin/Biotin Complex (ABC) (Vectorshields Labs,; Vectastain(R) ABC-HRP Kit, Peroxidase, PK-4000) diluted in PBS for 2 h at RT, and then washed with PBS before developing the sections with filtered diaminobenzidine (DAB tablets, sigma) for 1 min. The reaction was stopped by replacing the DAB solution with double distilled H_20, and then the sections were mounted to Fisher Superfrost plus gold slides and allowed to dry. Once tissue was adhered to the slides, it was dehydrated with increasing concentrations of ethanol and cleared with xylene. Glass coverslips were mounted to glass slides with Permount.

TABLE 1 Gene expression assays.

Gene	Gene Name	Assay ID	Source
Pycard	PYD and CARD domain containing (ASC)	Mm00445747_g1	ThermoFisher
Il1b	Interleukin 1 beta	Mm00434228_m1	ThermoFisher
Nlrp3	Nod like receptor-family, pyrin domain containing 3	Mm00840904_m1	ThermoFisher

Abbreviations: ASC, apoptosis-associated speck-like protein containing a CARD; NLR, (nucleotide-binding domain, leucine-rich repeat) and pyrin domain containing 3; PYCARD, (*N*-terminal pyrin-PAAD-DAPIN domain (PYD) and a C-terminal caspase-recruitment domain (CARD).

2.17 | Quantitative morphometry of Iba1 immunoreactivity

Images from AT180- and Iba1-labeled brain sections were captured on an Olympus BX-51 brightfield microscope through the magna-fire software and opened in FIJI/ImageJ (National Institutes of Health [NIH], USA). Files were converted into 8-bit images and automatically thresholded before the tool "Analyze particles" and "area fraction" tools used to record number and percentage of immunoreactivity $AT180^+$ and $Iba1^+$ cells in the cortex and CA1 regions.

2.18 | Microglia morphology using skeleton analysis (ImageJ)

Microglia analysis was performed on four separate images of the cortex in each mouse and averaged, and then captured on an Olympus BX-51. Briefly, images acquired from the microscope were processed with a bandpass filter, auto-corrected for brightness/contrast, auto-thresholded to focus on the darkest regions of the image, and de-speckled and converted into an 8-bit image file before transforming into a skeletonized figure, using the skeletonize.jar plugin NIH FIJI/ImageJ (as we described previously[29]).

2.19 | Quantitative real-time polymerase chain reaction (qRT-PCR)

RNA was extracted from rest of the hemi-brain (with minimal inclusion of cortex and hippocampus) using Trizol Reagent, as described by the manufacturer, and quantified via Nanodrop 2000. Total RNA was standardized (100 ng/µL), reverse transcribed into complimentary DNA using the High-Capacity cDNA Reverse transcription kit, amplified using TaqMan probes (Table 1), and normalized to eukaryotic 18S ribosomal RNA. Relative Quantification (RQ, $2^{-\Delta\Delta Ct}$) was calculated from the cycle threshold and these numbers were plotted in a heatmap using the Bioconductor package on R studio.

2.20 | Statistical analysis and study blinding

Statistical analysis was performed using GraphPad Prism (USA) software. Student's *t*-test was employed for two group comparisons. A one-way ANOVA, with Tukey's post hoc test, was used for three or more group comparisons. Unless otherwise noted, data are presented as mean ± standard error of the mean (SEM). The respective figure legends include additional details of the group size and specific statistics or post hoc tests used.

Data was *Z*-scored and normalized (MATLAB), and these values were plotted in heatmaps generated using the Complex Heat Map in the Bioconductor package in R Studio for the CBC.

All experiments were performed using a unique pathology numbering system (for necropsy studies) to avoid any subjective bias. Experimenters were blinded to the subject's genotype and treatment during all the experiments in this study. The genotype and treatment information were revealed only after the analysis was completed.

2.21 | Experiments involving non-human primates (NHPs; *Macaca mulatta*)

2.21.1 | Ethical statement

All non-human primate (NHP) studies were performed at the California National Primate Research Center (CNPRC) at the University of California Davis (UC Davis). The CNPRC is accredited by the Association for Assessment and Accreditation of Laboratory Animal Care International (AAALAC). All animal husbandry procedures and sample collections were performed according to established standard operating procedures and were in compliance with the 2011 *Guide for the Care and Use of Laboratory Animals* provided by the Institute for Laboratory Animal Research and the recommendations of the Weatherall report. The study was approved by the Institutional Animal Care and Use Committee of UC Davis (protocol #21934).

2.21.2 | Non-human primates (NHPs)—*M. mulatta*

A total of six young adults (6.3 ± 0.6 years of age, mean ± SEM; 3F and 3 M; Table S1) rhesus macaques (*M. mulatta*) were used for the study. These animals were from the CNPRC breeding colony, which is negative for simian immunodeficiency virus, type D retrovirus, and simian T-cell lymphotropic virus type 1. Macaques were housed indoors in stainless steel cages (Lab Product, Inc.) the sizing of which was scaled to the size of each animal, as per national standards, and were exposed to a 12-h light/dark cycle, 64°F –84°F, and 30%–70% room humidity. Animals had free access to water and received commercial chow (high protein diet, Ralston Purina Co.) and fresh produce supplements. When necessary for immunizations and blood collection, animals were fasted overnight and immobilized with ketamine HCl (10 mg/kg, i.m.). Animals were euthanized at the end of the study with ketamine sedation, followed by an overdose of sodium pentobarbital (120 mg/kg, i.v.); this method is consistent with American Veterinary Medical Association recommendations.

2.21.3 | Immunization of rhesus macaques

Rhesus macaques were immunized with either Qβ ($n = 3$) or pT181-Qβ ($n = 3$) (Table S1) at time 0 (Prime) with two booster immunizations at 4 weeks and 20 weeks. Each dose was 50 μg in 200 μL, administered intramuscularly into the right quadriceps muscle.

2.21.4 | Blood collection from vaccinated rhesus macaques

At time points 0, 2, 4, 6, and 8-weeks, blood was collected via peripheral venipuncture. EDTA-anti-coagulated blood was collected for CBC analysis, flow cytometry, and isolation of plasma according to standard methods. Finally, blood tubes without anti-coagulant ("red-top tubes") were allowed to clot at RT and were then processed via centrifugation at 800 *g* for 10 min to collect serum for biochemistry analysis and downstream analysis of anti-pT181 antibody titers. All serum, plasma, and peripheral blood mononuclear cells (PBMC) samples were cryopreserved and shipped on dry ice to the laboratories for further analysis.

2.21.5 | CBC and clinical serum chemistry

Hematology profiling (CBC and blood biochemistry) was performed by the CNPRC Clinical Laboratories. For the CBC, electronic cell counts were performed on a Pentra 60C+ analyzer (ABX Diagnostics); differential cell counts were performed using Giemsa/Wright-Giemsa staining. Clinical serum chemistry panels were performed using a Beckman Coulter AU480 chemistry analyzer. The parameters analyzed (CBC with differentials, clinical serum chemistry), units, and results are presented in the Supplementary Materials.

2.21.6 | Flow Cytometry

Four-color flow cytometric analysis was performed to characterize lymphocyte populations in rhesus macaque blood. A single aliquot of EDTA-anti-coagulated whole blood was stained with antibodies to CD3, CD4, CD8, and CD20 (all from Becton Dickinson): peridinin chlorophyll protein (PerCP)–conjugated anti-human CD8 (clone SK1), fluorescein isothiocyanate-conjugated anti-human CD3 (clone SP34), phycoerythrin-conjugated anti-human CD4 (clone L200), and allophycocyanin-conjugated anti-human CD20 (clone L27). Red blood cells were lysed, and the samples were fixed by the Coulter Q-prep system (Coulter Corporation, Hialeah, FL, USA). Flow cytometry was performed on FAC Symphony A3 (Becton Dickinson). Lymphocytes were gated by forward and side light scatter and were then analyzed with FACSDiva version 8.0.1. CD4+ T lymphocytes, CD8+ T lymphocytes, NK cells, and B cells were defined as CD4 + CD3+, CD8 + CD3+, CD8 + CD3−, and CD20 + CD3− lymphocytes, respectively.

2.21.7 | Quantification of humoral response against pT181 in the sera of vaccinated NHPs

Anti-pT181 specific IgG titer was determined by end-point dilution ELISA, using the 16-mer tau peptide (pT181) as the antigen. Briefly, immulon-2 plates were incubated with 500 ng streptavidin (Thermo Fisher Scientific, catalog #434301) in pH 7.4 PBS overnight at 4°C. Following washing, SMPH was added to the wells at 1 µg/well and incubated for 2 h at RT. pT181 was added to the wells at 1 µg/well and incubated overnight at 4°C. The plate was subsequently blocked with 0.5% milk in PBS for 2 h. Four-fold dilutions of sera from vaccinated rhesus macaques from each time point were added to each well and incubated for 2.5 h. The wells were probed with HRP-conjugated goat anti-human secondary antibody (Jackson ImmunoResearch, catalog #109-035-088; 1:4000) for 1 h. The reaction was developed using TMB substrate (Thermo Fisher Scientific, catalog #34028) and stopped using 1% HCl. The reactivity of sera for the target antigen was determined by measuring OD_{450}. Wells with twice the OD_{450} of the background were considered to be positive, and the highest dilution with a positive value was considered the end-point dilution titer.

2.21.8 | Hematoxylin and eosin (H&E) staining

The brains (cortex and hippocampus) of vaccinated macaques were formalin-fixed and paraffin-embedded (FFPE) and processed for standard H&E staining to assess gross neuropathological/histological changes.

2.21.9 | Quanterix single-molecule analysis of pT181 and neurofilament light (NfL) in human and NHP plasma samples

The pT181 Tau V2 Plasma and NfL Plasma kits (single molecule array—Simoa) HD-X, Quanterix were utilized to measure the levels of plasma levels of pT181 and neuronal dysfunction/neurodegeneration in both human and vaccinated NHPs. The Simoa single molecule array platform is an ultrasensitive assay that can detect brain-derived proteins like pT181 and NfL at sub-femtomolar concentrations. Kit instructions were followed with no modifications. Briefly, plasma samples were allowed to come to RT and then centrifuged at 10,000 *g* for 5 min to remove any debris. Specimen samples, standard curve samples nd digital and analog controls were added at 85 µL/well nd 85 µL/well of specimen sera to each well of a 96-well Simoa plate, and the assay was run under standard conditions.

2.22 | Experiments involving human subjects

2.22.1 | Ethical statement

UNM's Institutional Review Board (IRB) has approved (protocol #15-106) for all human subject experiments, including participation in blood collection and neurocognitive assessment. We certify that the study was performed in accordance with the ethical standards as laid down in the 1964 Declaration of Helsinki and its later amendments.

2.22.2 | Human subjects with cognitively unimpaired, mild cognitive impairment (MCI), and neuropathologically diagnosed postmortem samples with AD

CSF, plasma, and serum samples from clinically diagnosed subjects with cognitively unimpaired or subjects with MCI recruited to UNM's Mark-Vascular contributions to Cognitive Impairment and Dementia (MarkVCID) and NIH-funded P30 New Mexico Alzheimer's Disease Research Center (NM ADRC) through the University of New Mexico Center for Memory (CMA) were used. A diagnosis of MCI was confirmed by the Montreal Cognitive Assessment (MoCA) administered by a gerontologist (Dr. Janice Knoefel), where a score above 26 was considered cognitively unimpaired. We assessed 10 patients, 5 diagnosed with MCI and 5 who were cognitively unimpaired healthy controls (HCs), age = 70.40 ± 1.208, MCI age = 69.40 ± 2.768 (mean ± SEM), with mixed gender. Blood was collected and clotted at RT and then centrifuged at 10,000 rpm to separate sera from whole blood. CSF was collected by lumbar puncture by a neurologist as described previously.[30,31] pT181 and NfL levels in the plasma were measured as described above using Quanterix Simoa assays. Given the limited number of patient samples, we assessed both male and female patients to address diversity, equity, and inclusion in our study but were unable to include patients from a variety of racial/ethnic and geographic backgrounds.

Neuropathologically diagnosed postmortem frozen brain tissue of a 79-year-old patient diagnosed with AD at the age of 65, Braak VI, was obtained from the National Centralized Repository for Alzheimer's Disease and Related Dementias (NCRAD) and used for immunoprecipitations followed by western blot, mass spectrometry, or Quanterix Simoa. Dr. Karen SantaCruz and Dr. Elaine Bearer (University of New Mexico, Department of Pathology) provided neuropathologically diagnosed formalin-fixed AD brain tissue sections for immunohistochemical analyses.

2.22.3 | Immunoprecipitation of pT181 from human AD brains using pT181 vaccinated mice sera

The mice sera were obtained from mice vaccinated with Qβ scaffolds and pT181-coupled Qβ scaffolds. IgG antibodies were purified from the mice sera using Dynabeads Protein G partitioning in 1X PBS at 4°C overnight, followed by washing the unbound IgG from the magnetic beads. The bound IgG antibodies were eluted with 0.1 M glycine, pH 2.7, and neutralized in 1 M tris buffer, pH 8. After quantification of the protein content using BCA assay, the purified IgG antibodies were crosslinked on the Protein A/G using Pierce crosslinking IP/Co-IP kit. Forty micrograms of brain lysate, obtained from a 79-year-old

patient with Alzheimer's disease (Braak VI), was loaded as an input. Immunoprecipitation was performed by following the manufacturer's protocol, which was slightly modified at the elution step by using denaturing reagents to elute the bound target protein (pT181) under the heating condition at 95°C for 15 min before performing loading onto a 4%–12% Bis-Tris mini gel and running at 100 V for 1 h. The band intensity of anti-Tau5-HRP (1:5000, BioLegend Cat. No. 806405) was evaluated by western blot analysis, and the percentage of tau recovery was calculated from the immunoprecipitation/input.

3 | RESULTS

3.1 | Two doses of pT181-Qß vaccination show strong immunogenicity in the PS19 mouse model of tauopathy

To construct our VLP vaccine, we first synthesized a 13-mer peptide from the human MAPT sequence, which included a phosphorylated threonine at aa 181 (pT181) position (^{175}TPPAPKp**T**PPSSGEGGC^{190}), with numbering based on the human full-length tau with 441 aa sequence as described previously.[11] Next, we conjugated this peptide to the VLPs derived from Qß bacteriophage (Figure 1A). For efficient cross-linking of the pT181 peptide to surface-exposed lysine residues of the Qß bacteriophage, the C-terminal end of the pT181 peptide was modified by adding three additional amino acids (Gly-Gly-Cys) and conjugated to the Qß VLPs using a bifunctional crosslinker (SMPH; Figure 1A).[11] SDS-PAGE measured conjugation efficiency; successful peptide conjugation is indicated by an increase in the molecular weight of Qß coat protein subunits, reflecting conjugation of one or more peptides to the coat protein (Figure 1B). These results suggest that an average of >200 peptides are displayed on each VLP (Figure 1B).

The PS19 mouse model of tauopathy expresses human tau with *P301S* mutation and shows progressive tau pathology and cognitive impairment at about 6 months, which worsens as the mice age.[21] The 3.5-month-old PS19 and non-transgenic C57Bl/6j mice received two doses of pT181-Qß or Qß alone (control), administered 4 weeks apart. Serum anti-pT181 antibody titers were assessed after the first dose (at 4 months of age) and at ≈9 months of age. A CBC was performed at 6 months of age. Behavioral, biochemical, and histological analyses were conducted at ≈9 months of age. Figure 1A shows the experimental timeline. As expected, and as previously published,[11] robust anti-pT181 antibody titers were detected in the sera of 4-month PS19 mice following a single dose of pT181-Qß, but not in the Qβ vaccinated controls (Figure 1C). This antibody response was long-lasting, as significantly elevated titer persisted even up to 9months of age (Figure 1C). A direct comparison of the antibody response between the 4- and 9-month-old time points did not show any statistically significant reduction in circulating anti-pT181 antibodies, suggesting a robust and durable anti-pT181 antibody response in vaccinated PS19 mice. A dilution curve analysis of anti-pT181 titers showed that the pT181 antibody in the pT181-Qß vaccinated animals was on the order of 10^3–10^4 range at both 4 and 9 months of age (Figure 1D).

3.2 | Anti-pT181 antibodies from pT181-Qß vaccination are reactive to pathological tau in human AD brain sections

To determine the specificity of the anti-pT181 antibody, we performed immunohistochemical analyses by evaluating the reactivity of mouse sera to neuropathologically diagnosed human AD brain sections. Antibodies in sera derived from pT181-Qß vaccinated mice were highly reactive to perinuclear and somatodendritic pTau. Still, they had minimal to no reactivity to dystrophic neurites or pTau structures within the neuritic plaque; unlike AT8, which was used as a positive control (Figure 1E), likely due to the epitope availability in these unique tau structures (see Discussion). Sera derived from Qß vaccinated mice did not react to pTau (Figure 1E).

3.3 | pT181-Qß vaccination reduced soluble pTau and insoluble NFTs without microglial activation in 9-month-old PS19 mice

To determine whether pT181-Qß vaccination has any effect on pTau levels in the brains of vaccinated PS19 mice, we assessed the levels of hyperphosphorylated tau in the hippocampi of immunized mice. Both AT180 positive (pT231$^+$) pTau and total human tau (Tau12$^+$) were significantly reduced in the detergent soluble hippocampal lysates in pT181-Qß vaccinated 9-month-old mice compared to those immunized with Qß control (Figure 2A,B). Levels of soluble pTau recognized explicitly by the antibody AT8 (pS199/pS202/pT205) or Tau5 (which recognizes both human and endogenous mouse tau) were not altered. In a separate, larger cohort of PS19 mice immunized with pT181-Qß following the same paradigm, we again observed significant reduction in AT180 positive (pT231$^+$) pTau and total human tau (Tau12$^+$), with nearly significant reduction in AT8 positive tau ($p = 0.07$) and a significant increase in Tau5$^+$ endogenous mouse tau (Figure S1).

To confirm the results of the Western blot, we performed immunohistochemical analyses on brain sections of vaccinated PS19 mice. The pT181-Qß vaccinated mice showed a reduction of AT180$^+$ neurons in both the hippocampus and cortex (Figure 2C). Notably, an apparent reduction in soma/dendritic immunoreactivity of AT180 in the CA1 region of the hippocampus and primary loss of dendritic pTau immunoreactivity in the cortex were observed (Figure 2C). Taken together these data suggest that two doses of pT181-Qβ is sufficient to induce targeted reduction of soluble pTau species, AT180 in the hippocampus and cortex.

Next, to determine whether pT181-Qβ could reduce insoluble NFTs, we performed a Sarkosyl insoluble assay in the detergent-insoluble fractions of the hippocampus. Analysis of Tau12$^+$ bands at 50 kDa in Sarkosyl soluble and insoluble fractions showed a 47% and 93% reduction in Tau12 positivity, respectively (Figure 2D), suggesting a robust reduction in Sarkosyl insoluble tau with pT181-Qß vaccination in 9-month-old PS19 mice. We confirmed this result by conducting a Gallyas silver stain on brain tissue sections. In PS19 mice vaccinated with pT181-Qß, there was a 40% reduction in the number of Gallyas

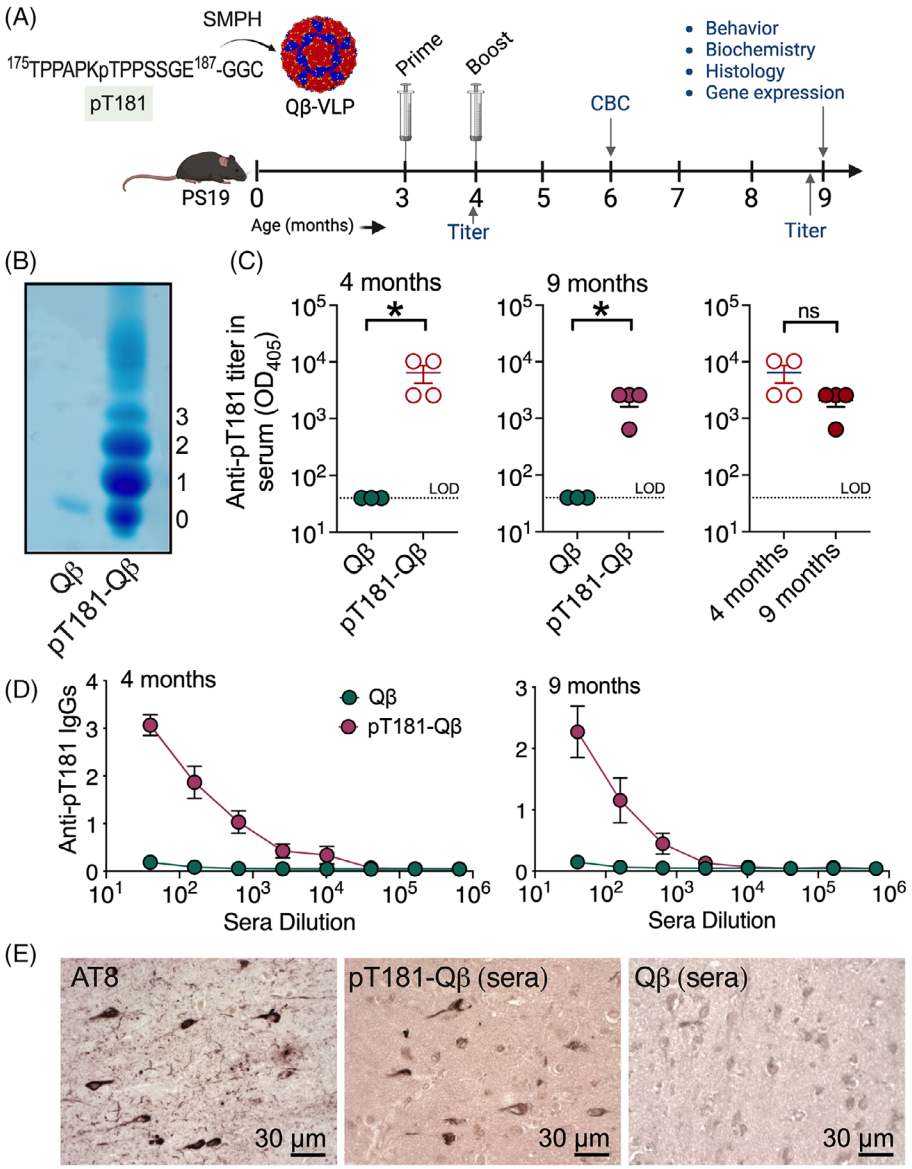

FIGURE 1 pT181-Qß vaccination induces a robust and long-lasting anti-pT181 tau antibody response. (A) 13-Mer peptides, including the phosphorylated epitope threonine 181 (pT181), were synthesized with two glycines (G) and a cysteine (C) and conjugated to the surface-exposed lysine residues on the coat proteins of a self-assembled Qß RNA bacteriophage (VLP) using a SMPH cross-linker. (B) Conjugation efficiency suggests that up to three peptides could be conjugated per coat protein (≈180 coat proteins/VLP x 3 = max 540 peptides/VLP). (C–D) Anti-pT181 IgG end-point titers (C) and serial dilutions (D) show that anti-pT181 IgGs remain significantly elevated until at least 9 months post-final immunization in PS19 mice. (E) Immune sera from pT181-Qß, but not Qß, vaccinated mice were reactive to pTau—similar to AT8, which was a positive control. LOD = limit of detection. Mean ± SEM, unpaired Student's *t*-test or one-way ANOVA, $^{*}p < .05$, $^{***}p < .005$; $n = 3$–4. Scale bar in E – 30 µm. ANOVA, Analysis of Variance; SMPH, Succinimidyl 6-[(beta-maleimidopropionamido) hexanoate].

silver-positive neurons in the entire cortical region (Figure 2E,F). These results suggest that pT181-Qß vaccination can significantly reduce mature NFTs in PS19 mice.

Finally, to determine if the antibodies generated from pT181-Q*β* vaccination induce microglial neuroinflammation through engagement/targeted reduction of soluble and insoluble pTau, we performed immunohistochemical analysis for the pan microglial marker, Iba1. Cortical Iba1 staining showed reactive microglia with swollen cell bodies and thicker processes only in Qß vaccinated 9-month-old PS19 mice but not in the PS19 that received pT181-Qß vaccination (Figure 2G).

Next we performed a quantitative skeleton analysis using ImageJ to determine the microglial architecture of Qß and pT181-Qß vaccinated PS19 mice (Figure 2H). Although the total number of Iba1^{+} cells/field was not altered between the two groups, we observed a significant decrease in the mean Iba1^{+} area/field in pT181-Qß vaccinated PS19 mice compared to Qß vaccinated PS19 controls. The mean Iba1^{+} area represents both the microglial cell body and processes that are reactive to Iba1 (Figure 2I). This analysis also revealed significantly increased endpoints (of microglial process), average branch length, and maximum branch length per microglial cell in the cortex of pT181-Qß vaccinated

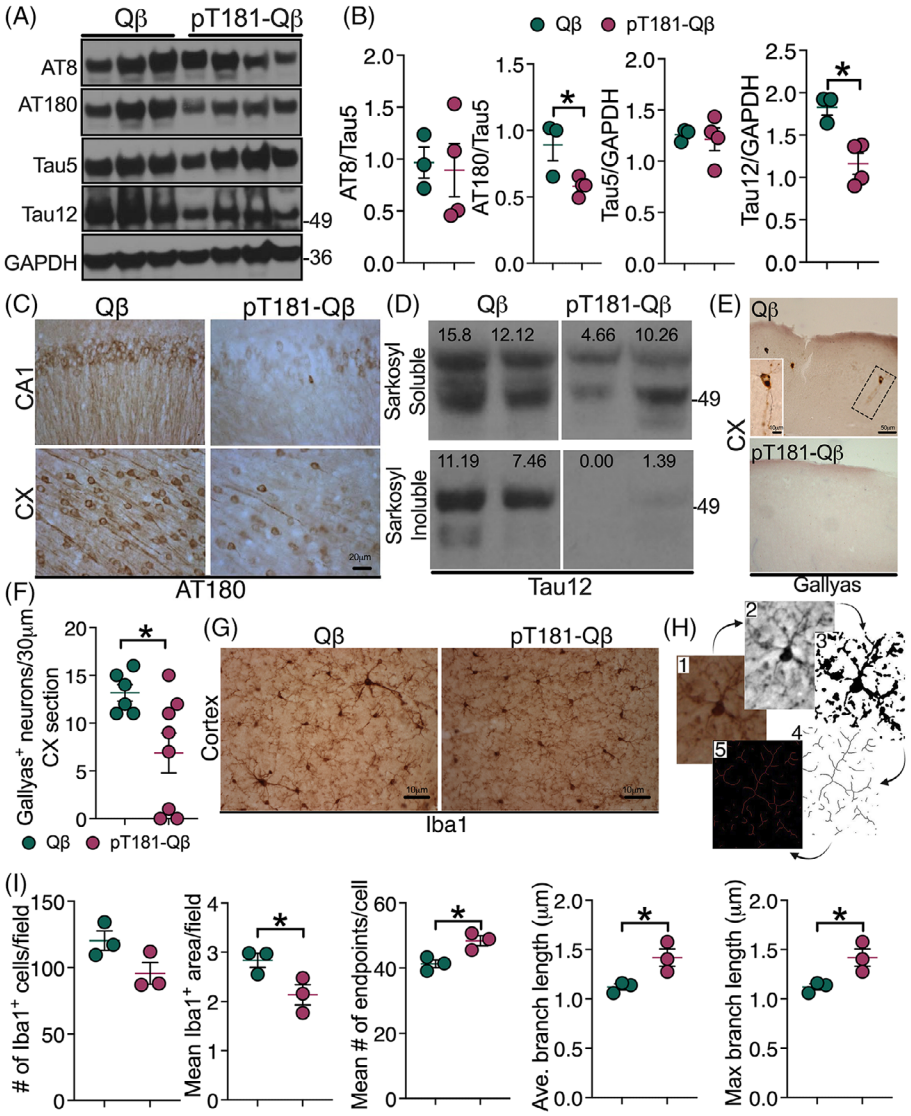

FIGURE 2 pT181-Qß vaccination reduces microgliosis, hyperphosphorylated and aggregated tau, and neuroinflammation in PS19 mice. (A–F) pT181-Qß vaccinated PS19 mice show reduced AT180$^+$ (pT231) site tau (A–B), Sarkosyl insoluble tau (D), and Gallyas silver positive NFTs (E) compared to PS19 mice vaccinated with Qβ alone. (G–I) Iba1$^+$ microglial morphology suggests reduced activation in 9-month-old PS19 mice vaccinated with pT181- Qß compared to Qß control. Mean ± SEM, unpaired Student's *t*-test, $^*p < .05$; $n = 3–5$.

PS19 mice compared to Qß vaccinated control PS19 mice (Figure 2I), indicating a classical morphology of homeostatic/resting microglia. Together, these results suggested that amelioration of pTau pathology in pT181-Qß vaccinated PS19 also reduced reactive morphological features of microglia.

To determine whether pT181-Qß vaccination has any adverse peripheral immune effects, we performed a CBC with differentials and a blood biochemistry panel in PS19 mice vaccinated with pT181-Qß compared to mice vaccinated with wild-type Qß or naïve, unvaccinated age-matched controls. There were no notable differences or discernable clustering patterns when we plotted all normalized and *Z*-scored data obtained from CBC and blood biochemistry panels for all vaccinated mice (Figure S2). We compared CBC and blood biochemistry profiles to age-matched non-transgenic unvaccinated controls. A few Qß-vaccinated PS19 mice showed a spike in markers such as neutrophils and red-cell distribution width. Still, they were not widespread among all treatment groups or statistically significant.

3.4 | pT181-Qß vaccination does not elicit an autoreactive T-cell response

A dual-color IL-4/IFN-γ Elispot assay was performed to assess for the presence of pT181-reactive or Qß VLP platform-reactive helper T cells in pT181-Qß vaccinated C57BL/6J mice. At 1-week after booster vaccinations with either unconjugated Qß or conjugated pT181-Qß VLPs, there was a significant elevation in the number of both IL-4 and IFN-γ spots compared to unvaccinated mice (Figure S3A-C). It is important to note that there was no significant difference in the number of IL-4 or IFN-γ spots between the pT181 or Qß stimulated T

cells and the vehicle-stimulated cells, indicating that vaccinating with VLPs stimulates a general helper T-cell response but does not elicit an antigen-specific T-cell response against the pT181 peptide or VLP platform (Figure S3B-C). At 5 weeks after the booster vaccination, there was no significant difference between the number of IL-4 or IFN-γ spots among the Qß or pT181-Qß and the unvaccinated control group, indicating that any T-cell response to the VLP vaccine is very short-lived and resolves within 5 weeks (Figure S3B-C). When comparing the ratio of IL-4 spots to IFN-γ spots to assess the Th2/Th1 index, we observed that both Qß and pT181- Qß VLP vaccination elicits a helper T-cell response that is strongly skewed in favor of the Th2 helper T-cell subset, which becomes even further skewed toward the Th2 helper T-cell subset between the 1-week and 5-week timepoints (Figure S3D).

3.5 | pT181-Qß vaccination reduced inflammasomes in 9-month-old PS19 mice

Next, we aimed to confirm whether the decreased activation of microglia in the brain leads to changes in the gene expression related to the inflammasomes, which are multi-protein complexes required for the maturation of IL-1β and IL-18.[32] This pathway plays a significant role in neuroinflammation and has been previously observed to be altered in both human and mouse models of tauopathy.[33,34] Furthermore, we have reported previously that these alterations can be mitigated through pT181-Qß vaccination in the rTg4510 mouse model of tauopathy.[20] Gene transcript levels for the messenger RNA (mRNA) of *Nlrp3* and *Pycard* (or apoptosis-associated speck-like protein containing acaspase activation and recruitment domain (ASC)), both critical components of the inflammasome complex, were significantly reduced in pT181-Qß vaccinated PS19 mice compared to Qß vaccinated PS19 controls (Figure S4). There was a >50% reduction in *Il1b* mRNA expression observed in pT181-Qß vaccinated PS19 mice compared with Qß vaccinated PS19 controls, which was not statistically significant due to variability in the Qß vaccinated group (Figure S4). Western blot analyses were conducted to assess the protein levels of these inflammasome components. Of interest, significantly reduced levels of inflammasome adaptor protein ASC, but not NLRP3 or caspase-1 (full length), were observed in pT181-Qß vaccinated PS19 mice compared with Qß vaccinated PS19 controls (Figure S4). These results suggest that anti-pT181 antibody-mediated neutralization of pTau also reduces inflammasome mRNA and protein (specifically ASC) levels in the brains of PS19 mice.

3.6 | pT181-Qß vaccination prevented cortical atrophy in PS19 mice

To determine if a reduction in pTau burden translates to improved brain structural integrity, we performed T2 volumetric 7T MRI analyses in PS19 mice immunized with pT181-Qß or, as a control, with Qß. First, Using the Allen Brain Atlas as a reference, we manually delineated ROIs for the cerebellum (control region), cortex, hippocampus, striatum, corpus callosum, and ventricles on coronal T2 MRI slices (n = 24 slices per mouse brain, Figure 3A-B). We observed a significant increase in the volume of cortex in the anatomic T2 MRI scan in pT181-Qß vaccinated PS19 mice compared with Qß vaccinated controls (Figure 3C). Similarly, the hippocampal volume was slightly larger, although not significantly so, in the pT181-Qß vaccinated PS19 mice. Conversely, the ventricular volumes were reduced, although this change was statistically significant (Figure 3C). The control regions (striatum and cerebellum), which are not affected in PS19 mice, did not show any significant difference between pT181-Qß vaccinated PS19 mice and Qß vaccinated controls (Figure 3C). Together, these results suggest that pT181-Qß vaccination not only reduces tau pathology but also prevents cortical atrophy in PS19 mice.

3.7 | pT181-Qß vaccination improved delay-dependent recognition memory in PS19 mice

PS19 mice show sex-specific and age-dependent cognitive impairment, motor dysfunction, and functional issues, with males showing more pronounced pathological changes than females.[35] However, both males and females have substantial cognitive and motor impairment by 7.5 months of age.[36] To determine whether pT181-Qß vaccination has any effect on cognitive and motor functions in PS19 mice, pT181-Qß vaccinated and Qß vaccinated PS19 mice were subjected to the NOR test and CatWalk analyses. Neither pT181-Qß nor Qß vaccinated PS19 mice showed a significant difference in velocity, total distance traveled (Figure S5), or the frequency of nose pokes to two identical objects (Figure 4A) in the NOR test during the sample day and were similar to non-transgenic controls. On the test day, pT181-Qß vaccinated PS19 mice spent significantly more time with the novel object than the familiar object. In contrast, Qß vaccinated PS19 control mice spent equal time with both objects (Figure 4A), suggesting that vaccination with pT181-Qß improves recognition memory in PS19 mice. Next, we performed CatWalk analyses to assess the gait and motor coordination in vaccinated PS19 mice. Notably, the stride length of all four paws was significantly increased in pT181-Qß vaccinated PS19 mice compared to Qß vaccinated controls (Figure 4B). Representative graphical print and timing views of CatWalk showed disturbed stride length in Qß vaccinated PS19 control mice, which appeared normal in pT181-Qß vaccinated PS19 mice (Figure 4C). To assess the effects of pT181-Qß vaccination on long-term spatial memory, a separate cohort of pT181-Qß vaccinated PS19 mice were subjected to the Morris Water Maze task. During the probe trial, pT181-Qß vaccinated mice spent significantly more time in the target quadrant of the arena than the Qß vaccinated PS19 mice, indicating rescue of spatial memory deficits by pT181-Qß vaccination (Figure S1). These results suggest that vaccination with pT181-Qß improved both delay-dependent recognition memory, spatial memory, and motor coordination in 9-month-old PS19 mice.

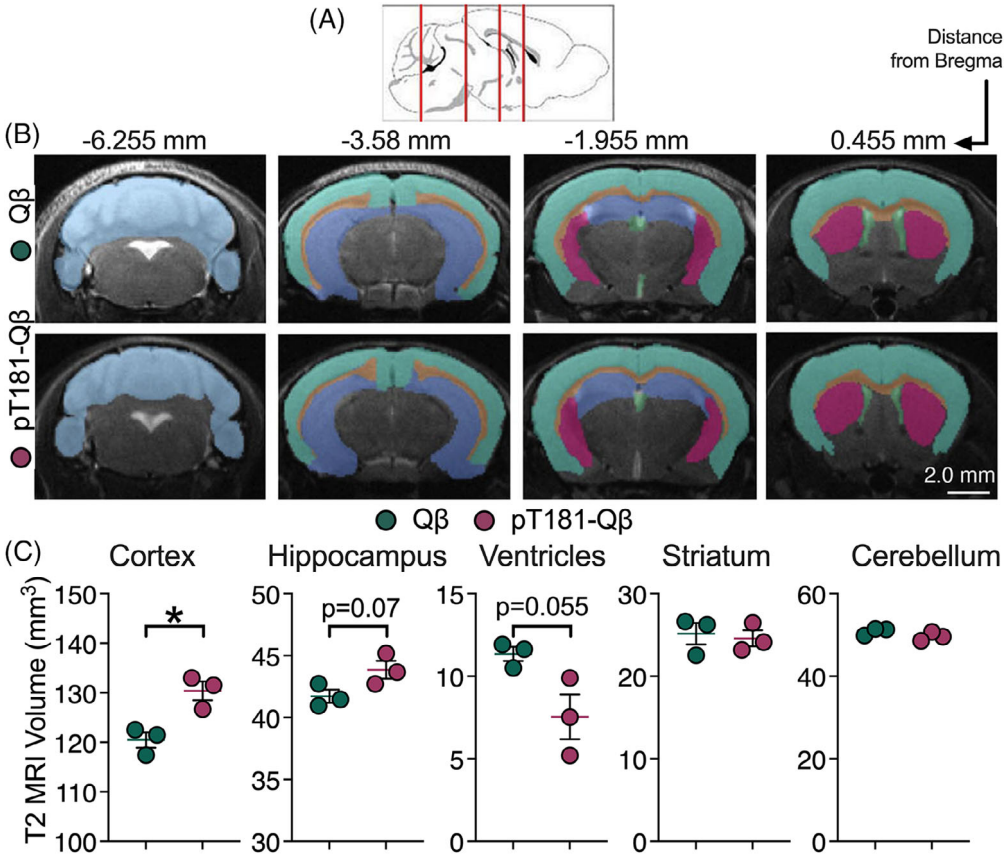

FIGURE 3 pT181-Qß vaccination reduces brain atrophy in PS19 mice. (A–C) T2-weighted MRI of the separate regions of interest (ROIs—cortical, aqua-cyan; hippocampal, dark blue; ventricle, green; striatum, pink; corpus callosum, light brown; and cerebellar, light blue) volumes shows prevention of brain atrophy in the cortex and a trend in the hippocampus. Corpus callosum quantification is not shown. Ventricle volumes are reduced in pT181-Qß vaccinated PS19 mice. Mean ± SEM, Student's *t*-test, $^*p < .05$, $n = 3–4$.

3.8 | hTau mice vaccinated with pT181-Qß showed a robust immune response, reduced pTau and ASC levels, and improved working memory

We have previously demonstrated the efficacy of pT181-Qß in the rTg4510 mouse model of tauopathy,[11,20] and the above results demonstrate effectiveness in the PS19 mouse model of tauopathy. These two mice represent a familial form of frontotemporal dementia and parkinsonism linked to chromosome-17 (FTDP-17) tauopathy, since they express mutated versions of human tau. Next, we wanted to determine whether pT181-Qß effectively reduces tau pathology in a mouse model tauopathy without any mutations in *MAPT* and is relevant to AD and other nonmutant tauopathies such as Pick's disease (PiD). We utilized the hTau mouse model, a genomic mouse model of human tau pathology (hTau), which expresses the entire human nonmutant tau (*MAPT*) gene with human regulatory elements[37] in a mouse tau deficient background.[24] These hTau mice exhibit age-related hyperphosphorylation and aggregation of tau,[24] synaptic abnormalities, cognitive impairment,[38] with evidence of subtle memory impairment as early as 6 months of age (as shown by others[39,40] and us[28]), and neuronal death.[23] Although the hTau mice express all six isoforms of human tau, the expression of 0N3R is the highest.[24] Therefore, hTau mice mimic the neuropathological aspects of PiD.[41]

The hTau mice were injected with two doses of pT181-Qß (or Qß control) at 6 and 7 months of age and assessed for the effectiveness of the vaccination at 12 months of age (Figure 5A) by performing Y-maze behavioral analyses to assess working memory and by performing biochemical analyses of brain lysates (Figure 5A). Anti-pT181 antibody titers were evaluated at 6.5 months and 12 months. As expected, pT181-Qß vaccinated hTau mice showed significantly elevated levels of anti-pT181 antibody titer compared to Qß vaccinated hTau control mice (Figure 5B,C), suggesting the durable and robust antibody response with only two doses of vaccination, as in the PS19 mice.

To determine if vaccination with pT181-Qβ reduced pathological tau, we performed western blot analyses in the hippocampal lysates of Qß or pT181-Qß vaccinated hTau mice. Similar to PS19 mice, pT181-Qß vaccination significantly reduced AT180$^+$ pTau. AT8$^+$ and PHF-1$^+$ (pS396/pS404) tau were decreased by 30%–40% compared to Qß vaccinated control hTau mice. Still, these differences were not statistically significant (Figure 5E). As we observed in PS19 mice, pT181-Qß vaccinated hTau mice also showed a significant three-fold reduction in ASC protein levels with no significant alteration in NLRP3 or Caspase-1 levels (Figure 5E), suggesting that the neutralization of pT181$^+$

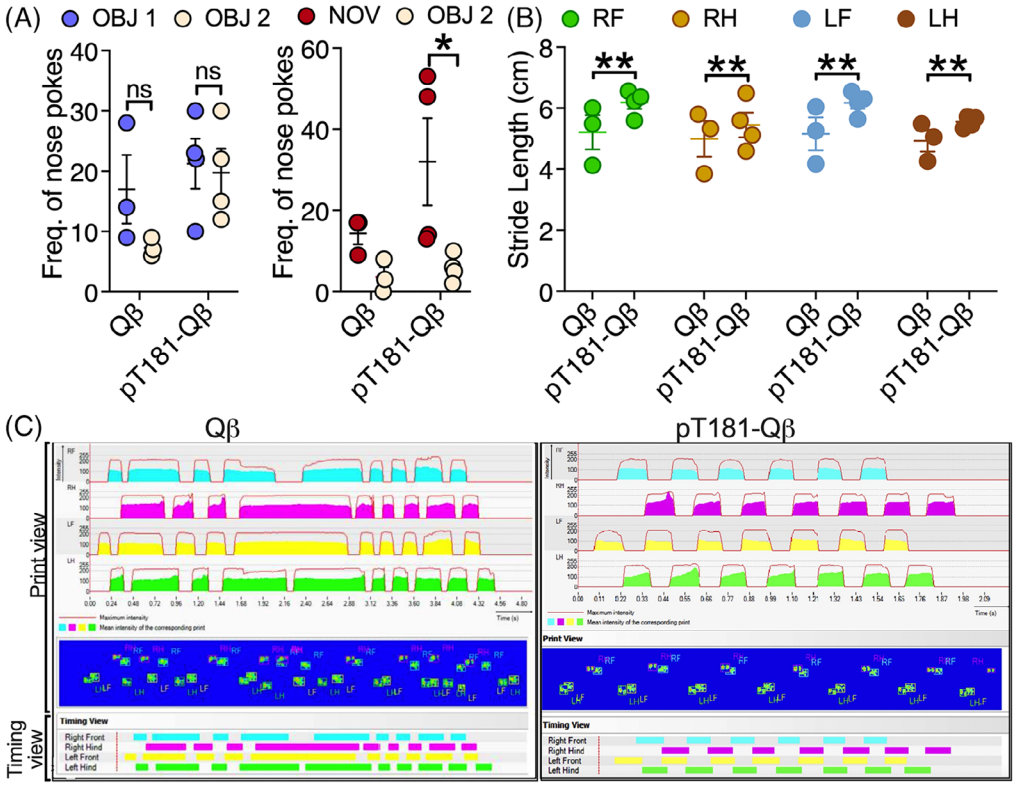

FIGURE 4 pT181-Qß vaccination improves delay-dependent memory and motor function in PS19 mice. (A) Frequency of nose pokes to the novel object (NOV) is increased in pT181-Qß vaccinated PS19 mice compared to controls on the test day (right graph. Left: no preference when tested them on identical objects [OBJ1 and OBJ2] on a training day). (B–C) Catwalk motor function test showing restoration of stride length on all four paws in pT181-Qß vaccinated PS19 mice. RF, right front paw; RH, right hind paw; LF, left front paw; LH, left hind paw. Mean ± SEM, Student's *t*-test. $^{*}p < .05$, two-way ANOVA, a Tukey's post hoc analysis was used, $^{**}p < .01$; $n = 3–4$.

tau reduces AT180^{+} tau and the inflammasome adaptor protein ASC. Finally, we performed a Y-maze test to assess whether the reduction in pTau in pT181-Qß vaccinated hTau mice translates to any cognitive recovery. We also measured the repeat ratio and spontaneous alternation in the pT181-Qß vaccinated hTau mice. There was an 8% improvement in spontaneous alternation (the sequence of arm entries for two arms was different than the previous arm/total arm entries) and a 31% reduction in repeat ratio in pT181-Qß vaccinated hTau mice (data not shown).

3.9 | Vaccination with pT181-Qß is safe and elicits strong tau-reactive antibody responses in NHPs

Qß VLP–based vaccines can elicit strong antibody responses in NHPs.[42–44] To evaluate the immunogenicity of pT181-Qß in primates, we vaccinated ≈6-year-old outbred rhesus macaques (*M. mulatta*). The safety of immunization and the ability to elicit human tau-reactive antibodies were also evaluated. Although healthy NHPs are not a model of tauopathy per se, recent results suggest that rhesus macaques have higher levels of NfL and pT181 compared to healthy human controls when both were processed with similar immune assays (personal communication, Dr. Marina Emborg). In addition, an age-dependent increase in the plasma levels of pT217^{+} tau has also been reported in NHPs.[7]

NHPs received three intramuscular immunizations (50 µg in 200 µL) with pT181-Qß ($n = 3$) or Qß control ($n = 3$), with the first two doses 4 weeks apart and the third at about 20 weeks after the first dose (Table S1). Blood was collected regularly prior to immunization till the end of the study. CSF was collected between 20 and 49 weeks (specifically at 20, 22, 24, 35, and 49 weeks) after the first dose, and necropsies were performed 49 weeks after the first prime dose (Figure 6A; Figure S6). Similar to what we observed in mouse models, pT181-Qß vaccination induced robust and statistically significant anti-pT181 antibody response in pT181-Qß vaccinated NHPs compared to those vaccinated with Qß controls (Figure 6B). The anti-pT181 IgG titers were measured through 49 weeks, and they stayed significantly elevated. Next, we measured the pT181 (antigen) in the plasma samples of vaccinated animals via Quanterix SIMOA pTau-181 Advantage V2 kit and determined that the levels of circulating pT181 showed a rapid drop after the second dose upon pT181-Qß vaccination (Figure 6C). Plotting the anti-pT181 antibody levels in the sera and pT181 antigen levels in the plasma showed an inverse correlation with reduction in plasma pT181 levels with increasing anti-pT181 antibody concentration in the sera from 2 through 8 weeks after the first prime injection (Figure 6D). Next, to determine the CNS bioavailability of anti-pT181 antibody, we

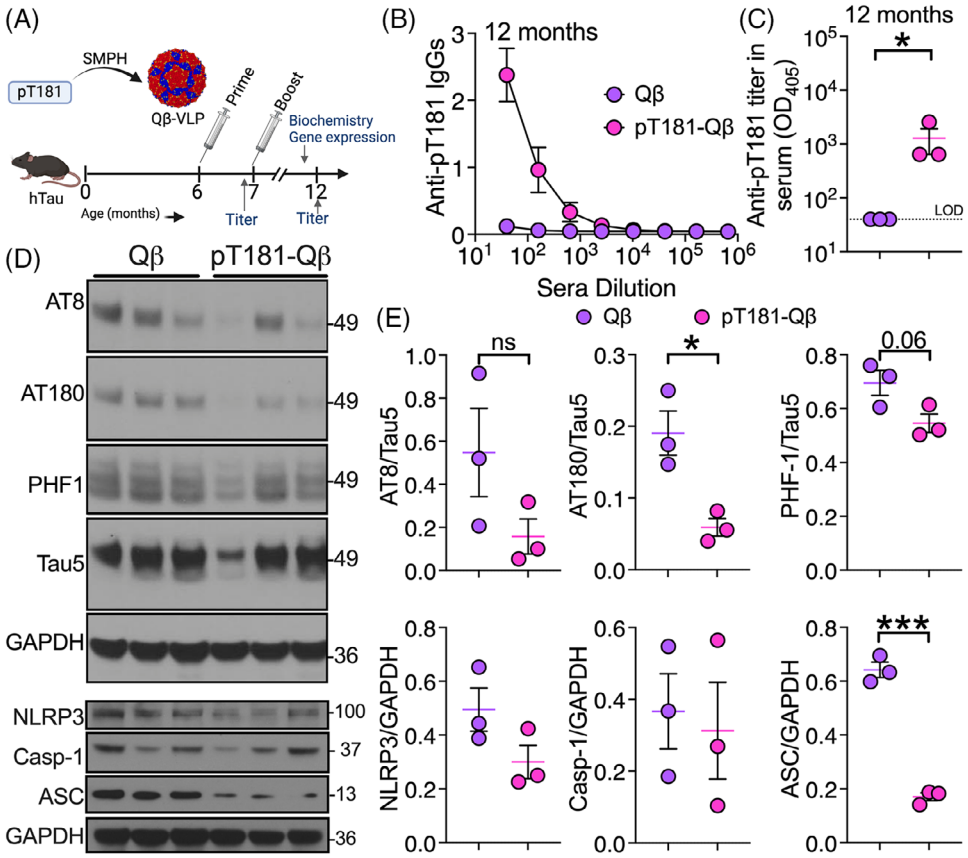

FIGURE 5 pT181-Qß vaccination is immunogenic, reduces pTau and inflammasome proteins, and rescues working memory in hTau mice. (A) Schematic showing the experimental timeline for pT181-Qß vaccination in hTau mice. (B–C) Anti-pT181 antibody dilution curve and antibody titers at 12-month time point. (D–E) pT181-Qß vaccination reduces AT180+ tau, PHF-1 (modestly), and inflammasome protein ASC in hTau mice. LOD = limit of detection. Mean ± SEM, Student's *t*-test. $^{*}p < .05$, $^{***}p < .005$; $n = 3$.

measured the anti-pT181 antibody levels in CSF at different time points between 20 and 49 weeks (Figure 6E). Following the second dose of pT181-Qβ, there was a significant increase in the amount of circulating anti-pT181 antibodies in the CSF at 20-, 22-, 24- and 49-week time points (Figure 6E), which suggest bioavailability of anti-pT181 antibody in the CNS of pT181-Qß vaccinated NHPs.

We next determined whether the anti-pT181 antibodies from NHPs were reactive to pathological tau in the brains of human AD. We have previously demonstrated that the sera from pT181-Qß vaccinated mice reacted specifically with pathological tau, similar to the reactivity of the commercial antibody AT8. As expected, sera from control Qβ vaccinated NHPs failed to show any specific labeling in human AD brain sections (Figure 6F). In contrast, immune sera from pT181-Qß vaccinated NHPs showed a staining pattern that was more typical of somatodendritic accumulation of pTau. This staining pattern was similar to the commerically available antibody AT8, though AT8 preferentially stained dystrophic neurites more abundantly than the pT181-Qß vaccinated NHP sera (Figure 6F). These data suggest that the anti-pT181 antibodies are reactive to pathogenic tau in human AD brain. However, the immunoreactivity pattern is slightly different from that of AT8—similar to those observed with mouse anti-pT181 immune sera.

To assess the safety of pT181-Qß vaccination in NHPs, similar to PS19 mouse experiments, we monitored the animal's overall health (including daily cage-side observations), regularly recorded body weights, and performed CBC with differentials, blood chemistry, as well as flow cytometric assessment of blood lymphocytes. Overall, animals had stable body weights and no evidence of any adverse effects. A list of hematological parameters and blood biochemistry markers are shown in Tables S2 and S5. For the blood parameters, although comparisons between both animal groups occasionally demonstrated a statistically significant difference of a parameter at a particular time point ($p < .05$) (Tables S2, S5; Figures S7–S12), they are not considered to have any biological significance because (1) with small group sizes ($n = 3$) and natural temporal variability of blood markers, occasional statistically significant differences are expected; (2) most values were within normal reference ranges; and (3) any values outside of the normal reference range were always minor, and changes were either sporadic and transient, or pre-existing (i.e., prior to first immunization). Most importantly, no observations in any of the blood parameters raised any clinical concerns for the veterinary staff.

Because we used healthy/relatively young NHPs in the current studies, we did not anticipate any significant AD/Alzheimer's disease and related dementias (ADRD)–related alterations. However, to

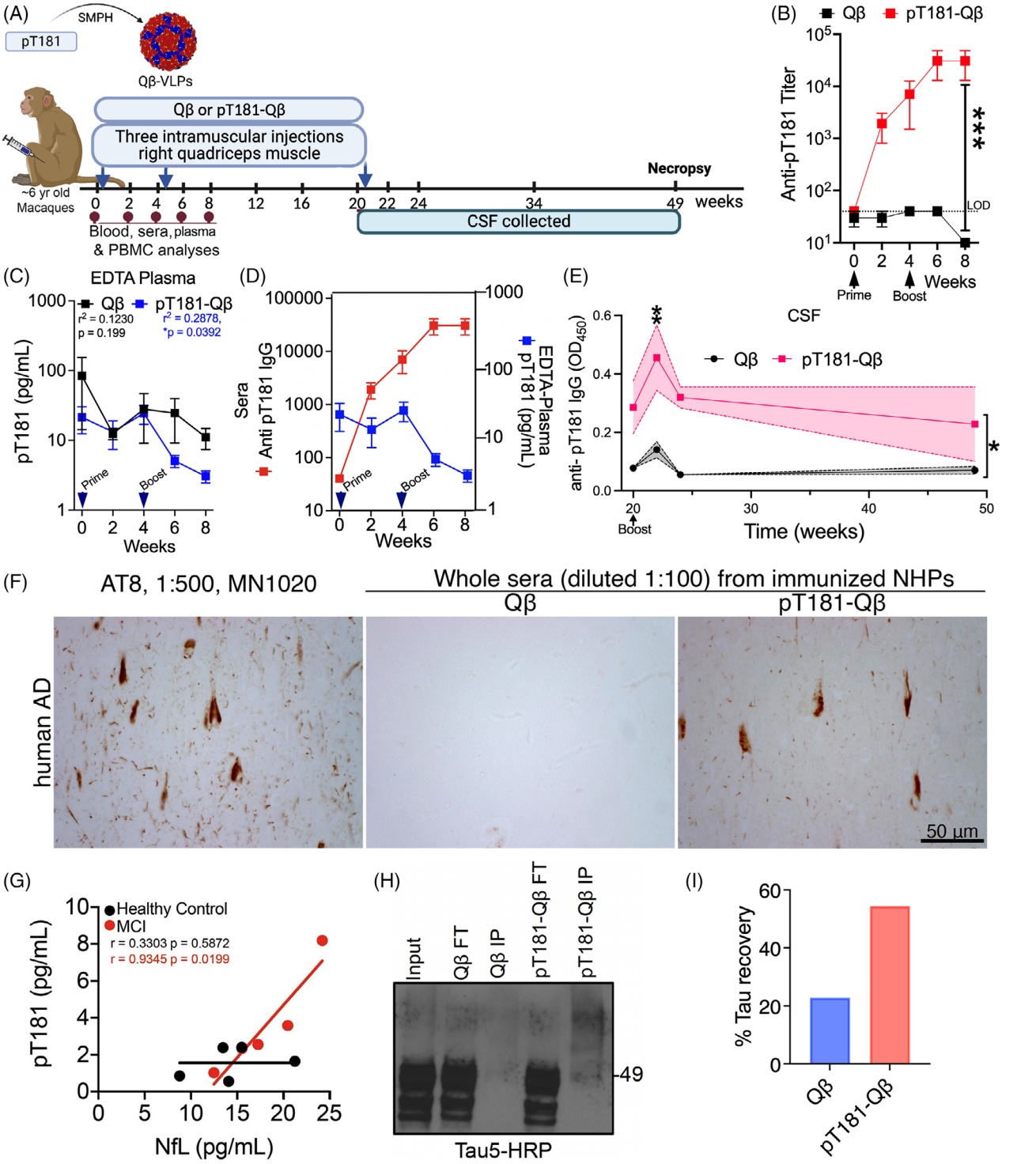

FIGURE 6 pT181-Qß vaccination in wild-type NHPs (*Macaca mulatta)* is immunogenic, shows target engagement, is detectable in the CSF, and is specific to pTau in the human brain. (A) Schematic showing the experimental timeline for pT181-Qß vaccination in ≈6-year-old macaques. (B) Anti-pT181 antibody titers at 8-week time point following vaccination. (C–D) Evidence of target engagement. Plasma pT181 levels (attributed to the age-related basal level of pT181) decrease with the increase in anti-pT181 body level in the sera at different time points following vaccination. € Anti-pT181 antibody levels in the CSF of NHPs and its dynamics at different time points following vaccination. (F) Anti-pT181 antibody from immunized macaque sera can detect pTau (similar to AT8, positive control) in human AD autopsy brain sections. (G) Plasma levels of pT181 (the target for pT181-Qß vaccination) are detectable in human patients with MCI compared to age-matched healthy controls recruited at the New Mexico Alzheimer's Disease Research Center. (H–I) Immunoprecipitation (IP) assay showing the Tau5^{+} bands and the % tau recovered from human AD brain lysates by the anti-pT181 IgGs from pT181-Qß vaccinated C57BL/6J mice. LOD = limit of detection. Mean ± SEM, Student's *t*-test or two-way ANOVA and a Tukey's post hoc analysis, $^{*}p < .05$, $^{**}p < .01$, $^{***}p < .005$; $n = 3$ pT181-Qß and $n = 3$ Qß. AD, Alzheimer's disease; NHPs, non-human primates; MCI, mild cognitive impairment.

TABLE 2 Details of human subjects used in the present study.

Patient ID	Diagnosis	MoCA score
#15-106A	AD	19
#15-106C	AD	22
#15-106E	AD	26
#15-106G	AD	14
#15-106i	AD	22
#15-106B	non-AD	25
#15-106D	non-AD	30
#15-106F	non-AD	29
#15-106H	non-AD	29
#15-106J	non-AD	27

MoCA, Montreal Cognitive Assessment.

determine whether vaccination was associated with any noticeable adverse cerebrovascular changes, hemorrhages, or meningitis in the brains of vaccinated animals, we performed hematoxylin and eosin (H&E) staining on tissue collected at necropsy after euthanasia. Based on the blinded analyses by two neuropathologists, all animals appeared normal without any notable changes in the H&E staining patterns in both pT181-Qß or Qß vaccinated NHPs (Figure S13). Together, these results suggest that the immune response induced by pT181-Qß was safe, with no significant adverse events noted in NHPs.

pT181 is present in the plasma of human MCI subjects and anti-pT181 antibody successfully engages the target (pT181 antigen) in human AD brain lysate

To determine whether antibodies from pT181-Qß vaccinated C57Bl/6j mice could engage the target (pT181), we first determined whether there were detectable levels of pT181 in the plasma samples of patients with MCI who were recruited into the NM ADRC (Table 2; human subjects with MoCA scores). As has been reported by numerous studies[5,45] and the NIH–Alzheimer's Association (AA; A+T+N+) criteria,[46] pT181 (mean ± SEM and in pg/ml of 3.53 ± 1.23 for MCI and 1.57 ± 0.38 for cognitively unimpaired subjects) was detectable in the plasma samples of subjects with MCI. pT181 levels correlated positively with the plasma levels of NfL (mean ± SEM and in pg/mL of 18.01 ± 2.02 for MCI and 14.59 ± 2.00 for cognitively unimpaired subjects), a marker of neuronal dysfunction,[45,47] in MCI subjects but not in cognitively unimpaired healthy individuals. These results are consistent with other reports indicating that pT181 is one of the earliest tau modifications in the MCI stage of dementia. Notably, our study did not recruit patients from a variety of racial/ethnic and geographical backgrounds and cannot address any variability among different human populations.

We next determined whether the anti-pT181 antibody from pT181-Qß vaccinated immune sera successfully engaged its target (pT181) by evaluating reactivity to human AD autopsy brain lysates. Conventional immunoprecipitations were done by incubating T-PER soluble AD brain lysates with the purified anti-pT181 IgG from Qß and pT181-Qß vaccinated C57Bl/6j mice and protein-A/G sepharose conjugated magnetic beads. The percentage of tau (by Tau5 antibody) recovered from human AD brain lysates with purified IgGs from pT181-Qß vaccinated C57Bl/6j mice was higher than that recovered with IgGs from Qß vaccinated C57Bl/6j mice (Figure 6H). These results suggest the engagement of pT181 (target) from human AD/ADRD brain lysates with anti-pT181 antibodies from pT181-Qß vaccinated C57Bl/6j mice.

4 | DISCUSSION

Here we describe the results on the immunogenicity, durability, safety, and efficacy of anti-pT181 tau antibodies upon pT181-Qß VLP vaccination in PS19 and hTau mouse models of tauopathy, as well as NHPs. In both PS19 and hTau mouse models, pT181-Qß vaccination induced a robust anti-pT181 antibody response, which was long-lasting and reactive to pathological tau in human AD brains. These antibodies were also safe and did not induce any notable adverse events, neuroinflammation, or alterations in the CBC profile. Notably, in both PS19 and hTau mice, the pT181-Qß vaccination specifically reduced pT231$^+$ (AT180 antibody site), total human tau, Sarkosyl insoluble, and Gallyas silver positive NFTs; prevented brain atrophy; and improved delay-dependent recognition memory and stride length in the Catwalk motor function test. Of interest, in both PS19 and hTau mice, pT181-Qß vaccination specifically reduced the levels of ASC, an essential adaptor protein required for the inflammasome assembly.

Similarly, NHPs vaccinated with pT181-Qß showed an encouraging safety profile. All vaccinated animals completed the entire study without any obvious overt clinical signs or showing any notable or clinically concerning changes in blood markers. Anti-pT181 antibodies were detectable in the CSF of vaccinated NHPs, suggesting the brain availability of anti-pT181 IgGs in vaccinated animals. Despite the NHPs being healthy, a low level of circulating pT181 was engaged by anti-pT181 antibodies, thereby showing an inverse correlation between the anti-pT181 IgG levels in the sera and pT181 antigen levels in the plasma in pT181-Qß vaccinated NHPs compared to controls. Finally, we showed that the anti-pT181 antibody could engage pT181 in the human patient's brain lysates and CSF samples.

Our results in these three animal models (PS19, hTau, and NHPs) corroborated our prior observations in rTg4510 tauopathy mice, a highly pathologically aggressive model of tauopathy.[11] pT181-Qß vaccination in rTg4510 mice showed robust and long-lasting antibody responses, a significant reduction in pathological tau levels, reduced brain atrophy, and improved synaptic integrity and memory.[11] Of interest, pT181-Qß vaccination in rTg4510 mice also reduced the levels of inflammasomes proteins, NLRP3 and ASC.[20] Thus the present study complemented several observations made in our previous studies but in two different mouse models of tauopathies (PS19 and hTau). Although we failed to detect a significant difference in AT8$^+$ and PHF1$^+$ tau and NLRP3 levels in the hTau model, this may be a result of insufficient statistical power of this study. Nevertheless, we consistently see significant reductions in tau pathology and inflammasome proteins across multiple disease models upon pT181-Qß vaccination.

The goals of the present study were to determine if the pT181-Qß vaccination was immunogenic, safe, and efficacious in additional animal models (PS19, hTau, and NHPs). Therefore, in-depth batteries of behavioral assessment and other functional studies were outside the scope of this study, and we have already reported in rTg4510 mice in our two prior studies.[11,20] Two novel aspects of the present study are the in-depth characterization of pT181-Qß vaccination in NHPs and full translatability of our findings between multiple species with target engagement of anti-pT181 antibodies in human brain lysates of human dementia cases. Based on this, we can confidently conclude that targeting pT181 via Qß VLP-based vaccination could be a viable approach to treating tauopathies.

Currently, there are no FDA-approved tau-targeted therapies for tauopathies. Tau aggregation inhibitors, anti-sense oligonucleotides, inhibitors of O-GlycNAcase (OGA), microtubule-stabilizing drugs, tau immunotherapies, and tau vaccines have been attempted in several pre-clinical models and clinical trials.[48,49] Fourteen tau therapeutics are being tested in various clinical trials[50] with varying efficacies, and data from these studies are slowly emerging. Despite varying results, tau immunotherapies appear to be relatively safe (unlike amyloid immunotherapies with amyloid-related imaging abnormalities [ARIA]) and have better clinically effective profiles.

We observed strong (≈10^4 end-point dilution titers) anti-pT181 antibody response in PS19, hTau mice, and NHPs, which were equivalent to the IgG response we observed in rTg4510 mice in our previous study.[11] These results suggest that irrespective of the mouse genetic background (PS19 and hTau were on C57BL/6j; and B6/FVB background in rTg4510), anti-pT181 antibody response upon pT181-Qß vaccination is comparable in mice and in NHPs. This is important considering the translatability of the pT181-Qß vaccination to humans with diverse backgrounds and demographics with varying abilities to elicit an immune response to a vaccine. In addition to similar response levels, it was also important to note that the circulating levels of anti-pT181 antibodies were detectable long after the second booster, suggesting highly durable immune responses to $pT181^+$ tau.

Of interest, anti-pT181 antibodies were reactive to pathological tau, mostly confined to the ghost tangles, perinuclear NFTs, and somatodendritic structures in the human AD brain. This differed from AT8 antibody reactivity, which detected neuropil threads and dystrophic neurites, and this difference could be due to the accessibility and the presence of pS199/pS202/pT205 (AT8) versus pT181 epitopes on the intraneuronal or extracellular pathological tau. The origin of pT181 likely occurs and stays intraneuronal, whereas the AT8 epitopes start in neurons and then move to dystrophic axons or dendrites. In support of this possibility, an earlier study has shown that tau oligomeric antibody T22 preferably stained only intraneuronal NFTs, whereas AT8 stained both intra- and extra-neuronal NFTs.[51] Alternatively, because AT8 has multiple epitopes (pS199, pS202, and pT205 as well as pS208)[52–54] and appears relatively late in the disease progression,[1,55–60] it could be possible that many more epitopes are accessible for AT8 than for anti-pT181 antibodies.

pT181-Qß vaccination significantly reduced detergent-soluble phosphorylated tau, Sarkosyl insoluble levels, and Gallyas silver-positive NFTs. Among the two phosphorylation sites (AT8 and AT180) studied, pT181-Qß vaccination significantly reduced the AT180, but not AT8, positive tau in both PS19 and hTau mice, but it is unclear why. We speculate that pT181-Qß vaccination may be efficient in reducing early pathological tau epitopes like AT180/pT231[6] but may not be efficient in reducing tau pathology in relatively advanced stages, especially when multiple pTau epitopes (AT8) emerge. Understanding the effect of pT181-Qß vaccination on various individual tau epitopes needs in-depth characterization in the future. It is also important to note that pT181-Qß vaccination primarily reduced $Tau12^+$ human tau, but not mouse tau, in PS19 mice, suggesting relative specificity to human tau. In addition to the Qß VLP platform, other antigen display platforms like Norovirus P-particle[61] and flagellin B adjuvanted[62] strategies have also shown immunogenicity and ameliorated tau pathology.

In PS19 mice, microglial activation precedes tau pathology, and suppression of inflammation by the immunosuppressive compound FK506, reduces hyperphosphorylated tau levels and enhances the longevity of PS19 mice.[21] We previously demonstrated that genetically enhancing microglial activation via deletion of CX3CR1 accelerated tau pathology and cognitive impairment in the hTau mouse model of tauopathy.[63] Additional mechanistic studies have suggested that microglia-driven tau pathology is mediated by interleukin-1ß (IL-1ß) signaling, which activates the neuronal p38 mitogen-activated protein kinase (p38 MAPK) pathway.[28,63,64] We also showed that blocking IL-1ß signaling via global and genetic knockout of inflammasomes adaptor protein ASC (apoptosis-associated speck-like protein containing a caspase recruitment domain [CARD]) reduced tau pathology and improved spatial memory, which is a consequence of reduced IL-1ß in hTau mice with myeloid-cell restricted deletion of ASC ($hTauCX3CR1CreASC^{f/f}$ mice).[20] Here we observed that neutralizing hyperphosphorylated tau with pT181-Qß vaccination reduced the number of activated microglia, restored their resting morphology, and mRNA and protein levels of ASC but not NLRP3. Strikingly, reduced ASC levels were observed upon pTau neutralization in hTau (Figure 6) and rTg4510 mice.[11] It is unclear why reducing pTau levels consistently reduced both mRNA and protein levels of ASC but not NLRP3. Future studies must understand how pTau neutralization affects different types of inflammasomes and their components. Nonetheless, based on our prior report[65] on the possibility of cross-seeding of pathological tau and inflammasomes (ASC specks), it is likely that reducing the level of one versus the other will lead to amelioration of neuroinflammation and tau pathology and vice versa. Here, our data further support the assertion from our previous report[65] that proteopathic tau serves as an inflammatory stimulus in the brain for both priming and activation of the NLRP3 inflammasome, which can be ameliorated by reducing tau pathology.

Consistent with mice studies, pT181-Qß vaccination in NHPs also induced a robust antibody response, which engaged basal levels of pT181 antigen in the plasma. It is notable that anti-pT181 antibodies were detected in the CSF of vaccinated NHPs. The CSF anti-pT181 antibody levels were found to be elevated after the second boost (at 20 weeks after the first prime injection) and stayed significantly higher

than the baseline at the 49-week time-point, when the experiment was terminated. It is uncertain what regulates the dynamics of antibody bioavailability in the CSF or brains of the vaccinated animals. However, our results suggest that even in relatively healthy animals, a substantial amount of anti-pT181 antibodies readily enter the CNS upon pT181-Qß vaccination, and these antibodies are specific to pathological tau aggregated in the human AD brain and CSF. We observed an excellent safety profile of pT181-Qß vaccination in NHPs.

In summary, we report a comprehensive characterization of pT181-Qß vaccination in two different (PS19 and hTau) mouse models of tauopathy and young-adult NHPs, which are ≈18 years in human years based on the 1:3 age ratio between macaques and humans.[66] pT181-Qß vaccination induced robust antibody responses, displayed favorable safety profile, and specifically reduced AT180^{+} phosphorylated tau, Sarkosyl insoluble, and Gallyas silver positive NFTs; improved delay-dependent recognition memory and motor function; as well as prevented brain atrophy. These results suggest that pT181 is a potential therapeutic target for tauopathies.

AUTHOR CONTRIBUTIONS

Kiran Bhaskar, Nicole M. Maphis, and Bryce Chackerian designed experiments. Nicole Maphis, Jonathan Hulse, Suttinee Poolsup, and Somayeh Dadras performed most of the experiments. Manas Kandath and Madelin J Whelpley assisted with brain sectioning and IHC. Julianne Peabody performed all titer analyses; Manas Kandath, Colin Wilson, and Reed Selwyn performed/assisted with the magnetic resonance imaging analyses. Jeff Thompson and Sasha Hobson provided human cerebrospinal fluid and plasma samples that Gary Rosenberg, Kiran Bhaskar, and Janice Knoefel oversee as a part of Biomarkers for Vascular Contributions to Cognitive Impairment and Dementia (MarkVCID) and New Mexico Alzheimer's disease research consortium (NM ADRC) studies. Danielle Beckman, Sean P Ott, Jennifer W. Watanabe, Jodie L. Usachenko, Koen K Van Rompay, and John Morrison performed all nonhuman primate studies. Gary Rosenberg and Janice Knoefel are clinicians and assisted in providing blood and CSF samples from clinically diagnosed subjects. Kiran Bhaskar, Jonathan Hulse, and Nicole Maphis drafted/edited the manuscript. All authors have read and approved the manuscript.

ACKNOWLEDGMENTS

We thank Ms. Devon Chisholm, Ms. Tram Le, and the entire ARF facility at UNM for genotyping, animal husbandry, and genotyping. We thank Irina Ms. Lagutina from the Animal Models Shared Resource Core for blood collection and subsequent CBC/blood biochemistry analysis. Thanks to Dr. Russ Morton and Dr. Carissa Miliken, the preclinical core (PCC) in the Center for Brain Recovery and Repair (CBRR) performed Catwalk and other behavioral studies. We thank Dr. Yirong Yang for initiating the MRI studies and helping with data analyses. Dr. Lea Weston provided the macro code for Skeletonize. We thank Dr. David Linsenbardt for the R studio and Matlab help. We thank Drs. Karen SantaCruz and Elaine Bearer for providing human autopsy AD brain sections for immunohistochemistry. We thank the staff of CNPRC Colony Management and Research Services, Clinical Laboratories, Anatomic and Clinical Pathology, and Veterinary staff for their expert technical assistance with the nonhuman primate studies. This study was supported by (1)RF1NS083704-05A1, R01NS083704, New Mexico Higher Education Department Technology Enhancement Fund (TEF), University of New Mexico (UNM) Health Sciences Center Bridge Support, UNM Department of Molecular Genetics and Microbiology intradepartmental grant, the New Mexico Alzheimer's Disease Research Center (NM ADRC) P30 grant P30AG086404-01 funding; a CNPRC Pilot Program Award (to K.B.) and Award P51OD011107 from the Office of Research Infrastructure Program, Office of The Director, National Institutes of Health to the California National Primate Research Center. (2) UNM Center for Biomedical Research Excellence (CoBRE) in Center for Brain Recovery and Repair Pre-Clinical Core P20GM109089. Autophagy, Inflammation, and Metabolism (AIM) CoBRE Center P20GM121176-04. (3) Dr. Stephanie Ruby's travel award (to N.M. and J.H.), a T32 training grant (to J.H), as well as the Institutional Research and Academic Career Development Award (IRACDA # NIH, K12GM088021) post-doctoral fellowship and NIH Research Evaluation and Commercialization Hubs (REACH) Loan Repayment Program Grant (to N.M). (4) Samples from the National Centralized Repository for Alzheimer's Disease and Related Dementias (NCRAD), which receives government support under a cooperative agreement grant (U24AG21886) awarded by the National Institute on Aging - MarkVCID-II were used in this study. The content is solely the responsibility of the authors and does not necessarily represent the official views of the NIH.

CONFLICT OF INTEREST STATEMENT

The authors declare no competing interests or conflicts. Author disclosures are available in the Supporting Information.

CONSENT STATEMENT

All human subjects provided written informed consent prior to the study.

REFERENCES

1. Neddens J, Temmel M, Flunkert S, et al. Phosphorylation of different tau sites during progression of Alzheimer's disease. *Acta Neuropathol Commun*. 2018;6:52.
2. Wesseling H, Mair W, Kumar M, et al. Tau PTM profiles identify patient heterogeneity and stages of Alzheimer's disease. *Cell*. 2020;183:1699-1713.e13.
3. Kivisakk P, Carlyle BC, Sweeney T, et al. Plasma biomarkers for diagnosis of Alzheimer's disease and prediction of cognitive decline in individuals with mild cognitive impairment. *Front Neurol*. 2023;14:1069411.
4. Gobom J, Benedet AL, Mattsson-Carlgren N, et al. Antibody-free measurement of cerebrospinal fluid tau phosphorylation across the Alzheimer's disease continuum. *Mol Neurodegener*. 2022;17:81.
5. Karikari TK, Emersic A, Vrillon A, et al. Head-to-head comparison of clinical performance of CSF phospho-tau T181 and T217 biomarkers for Alzheimer's disease diagnosis. *Alzheimers Dement*. 2021;17:755-767.
6. Mila-Aloma M, Ashton NJ, Shekari M, et al. Plasma p-tau231 and p-tau217 as state markers of amyloid-beta pathology in preclinical Alzheimer's disease. *Nat Med*. 2022;28:1797-1801.
7. Datta D, Perone I, Wijegunawardana D, et al. Nanoscale imaging of pT217-tau in aged rhesus macaque entorhinal and dorsolateral prefrontal cortex: evidence of interneuronal trafficking and

early-stage neurodegeneration. *Alzheimers Dement*. 2024;20(4):2843-2860. doi:10.1002/alz.13737
8. West T, Hu Y, Verghese PB, Bateman RJ, et al. Preclinical and clinical development of ABBV-8E12, a humanized anti-tau antibody, for treatment of Alzheimer's disease and other tauopathies. *J Prev Alzheimers Dis*. 2017;4:236-241.
9. Novak P, Schmidt R, Kontsekova E, et al. FUNDAMANT: an interventional 72-week phase 1 follow-up study of AADvac1, an active immunotherapy against tau protein pathology in Alzheimer's disease. *Alzheimers Res Ther*. 2018;10:108.
10. Theunis C, Crespo-Biel N, Gafner V, et al. Efficacy and safety of a liposome-based vaccine against protein tau, assessed in tau.P301L mice that model tauopathy. *PloS one*. 2013;8:e72301.
11. Maphis NM, Peabody J, Crossey E, et al. Qß Virus-like particle-based vaccine induces robust immunity and protects against tauopathy. *NPJ vaccines*. 2019;4:26.
12. Chackerian B, Peabody DS. Factors that govern the induction of long-lived antibody responses. *Viruses*. 2020;12:74.
13. Mohsen MO, Bachmann MF. Virus-like particle vaccinology, from bench to bedside. *Cell Mol Immunol*. 2022;19:993-1011.
14. Vanderstichele H, De Vreese K, Blennow K, et al. Analytical performance and clinical utility of the INNOTEST PHOSPHO-TAU181P assay for discrimination between Alzheimer's disease and dementia with Lewy bodies. *Clin Chem Lab Med*. 2026;44(12):1472-1480. doi:10.1515/CCLM.2006.258
15. Saman S, Kim W, Raya M, et al. Exosome-associated tau is secreted in tauopathy models and is selectively phosphorylated in cerebrospinal fluid in early Alzheimer disease. *J Biol Chem*. 2012;287:3842-3849.
16. Holmes BB, Devos SL, Kfoury N, et al. Heparan sulfate proteoglycans mediate internalization and propagation of specific proteopathic seeds. *Proc Natl Acad Sci U S A*. 2013;110:E3138-47.
17. Kanmert D, Cantlon A, Muratore CR, et al. C-Terminally truncated forms of tau, but not full-length tau or its C-terminal fragments, are released from neurons independently of cell death. *J Neurosci*. 2015;35:10851-10865.
18. Wray S, Saxton M, Anderton BH. Hanger DP. Direct analysis of tau from PSP brain identifies new phosphorylation sites and a major fragment of N-terminally cleaved tau containing four microtubule-binding repeats. *J Neurochem*. 2008;105:2343-2352.
19. Yang CC, Chiu MJ, Chen TF, Chang HL, Liu BH, Yang SY. Assay of plasma phosphorylated tau protein (Threonine 181) and total tau protein in early-stage Alzheimer's disease. *J Alzheimers Dis*. 2018;61:1323-1332.
20. Jiang S, Maphis NM, Binder J, et al. Proteopathic tau primes and activates interleukin-1beta via myeloid-cell-specific MyD88- and NLRP3-ASC-inflammasome pathway. *Cell Rep*. 2021;36:109720.
21. Yoshiyama Y, Higuchi M, Zhang B, et al. Synapse loss and microglial activation precede tangles in a P301S tauopathy mouse model. *Neuron*. 2007;53:337-351.
22. Maphis NM, Jiang S, Binder J, et al. Whole genome expression analysis in a mouse model of tauopathy identifies MECP2 as a possible regulator of tau pathology. *Front Mol Neurosci*. 2017;10:69.
23. Andorfer C, Acker CM, Kress Y, Hof PR, Duff K, Davies P. Cell-cycle reentry and cell death in transgenic mice expressing nonmutant human tau isoforms. *J Neurosci*. 2005;25:5446-5454.
24. Andorfer C, Kress Y, Espinoza M, et al. Hyperphosphorylation and aggregation of tau in mice expressing normal human tau isoforms. *J Neurochem*. 2003;86:582-590.
25. Dawson HN, Ferreira A, Eyster MV, Ghoshal N, Binder LI, Vitek MP. Inhibition of neuronal maturation in primary hippocampal neurons from tau deficient mice. *J Cell Sci*. 2001;114:1179-1187.
26. Crossey E, Amar MJ, Sampson M, et al. A cholesterol-lowering VLP vaccine that targets PCSK9. *Vaccine*. 2015;33:5747-5755.
27. Akache B, Weeratna RD, Deora A, et al. Anti-IgE Qb-VLP conjugate vaccine self-adjuvants through activation of TLR7. *Vaccines*. (Basel). 2016;4(1):3. doi:10.3390/vaccines4010003
28. Maphis N, Xu G, Kokiko-Cochran ON, et al. Reactive microglia drive tau pathology and contribute to the spreading of pathological tau in the brain. *Brain*. 2015;138:1738-1755.
29. Weston LL, Jiang S, Chisholm D, Jantzie LL, Bhaskar K. Interleukin-10 deficiency exacerbates inflammation-induced tau pathology. *J Neuroinflammation*. 2021;18:161.
30. Hillmer L, Erhardt EB, Caprihan A, et al. Blood-brain barrier disruption measured by albumin index correlates with inflammatory fluid biomarkers. *J Cereb Blood Flow Metab*. 2023;43:712-721.
31. Sanchez KE, Jiang S, Palencia Desai S, et al. Protocol to measure apoptosis-associated speck-like protein containing a CARD specks in human cerebrospinal fluid via imaging flow cytometry. *STAR Protoc*. 2024;5:102916.
32. Fu J, Wu H. Structural mechanisms of NLRP3 inflammasome assembly and activation. *Annual review of immunology*. 2023;41:301-316.
33. Ising C, Venegas C, Zhang S, et al. NLRP3 inflammasome activation drives tau pathology. *Nature*. 2019;575:669-673.
34. Venegas C, Kumar S, Franklin BS, et al. Microglia-derived ASC specks cross-seed amyloid-beta in Alzheimer's disease. *Nature*. 2017;552:355-361.
35. Sun Y, Guo Y, Feng X, et al. The behavioural and neuropathologic sexual dimorphism and absence of MIP-3alpha in tau P301S mouse model of Alzheimer's disease. *J Neuroinflammation*. 2020;17:72.
36. Lasagna-Reeves CA, de Haro M, Hao S, et al. Reduction of Nuak1 decreases tau and reverses phenotypes in a tauopathy mouse model. *Neuron*. 2016;92:407-418.
37. Duff K, Knight H, Refolo LM, et al. Characterization of pathology in transgenic mice over-expressing human genomic and cDNA tau transgenes. *Neurobiol Dis*. 2000;7:87-98.
38. Polydoro M, Acker CM, Duff K, Castillo PE, Davies P. Age-dependent impairment of cognitive and synaptic function in the htau mouse model of tau pathology. *J Neurosci*. 2009;29:10741-10749.
39. Geiszler PC, Barron MR, Pardon MC. Impaired burrowing is the most prominent behavioral deficit of aging htau mice. *Neuroscience*. 2016;329:98-111.
40. Phillips M, Boman E, Osterman H, Willhite D, Laska M. Olfactory and visuospatial learning and memory performance in two strains of Alzheimer's disease model mice–a longitudinal study. *PloS one*. 2011;6:e19567.
41. Denk F, Wade-Martins R. Knock-out and transgenic mouse models of tauopathies. *Neurobiol Aging*. 2009;30:1-13.
42. Crossey E, Amar MJA, Sampson M, et al. A cholesterol-lowering VLP vaccine that targets PCSK9. *Vaccine*. 2015;33:5747-5755.
43. Fowler A, Van Rompay KKA, Sampson M, et al. A virus-like particle-based bivalent PCSK9 vaccine lowers LDL-cholesterol levels in non-human primates. *NPJ vaccines*. 2023;8:142.
44. Jelinkova L, Jhun H, Eaton A, Petrovsky N, Zavala F, Chackerian B. An epitope-based malaria vaccine targeting the junctional region of circumsporozoite protein. *NPJ vaccines*. 2021;6:13.
45. Janelidze S, Mattsson N, Palmqvist S, et al. Plasma P-tau181 in Alzheimer's disease: relationship to other biomarkers, differential diagnosis, neuropathology and longitudinal progression to Alzheimer's dementia. *Nat Med*. 2020;26:379-386.
46. Jack CR Jr, Andrews JS, Beach TG, et al. Revised criteria for diagnosis and staging of Alzheimer's disease: Alzheimer's Association Workgroup. *Alzheimers Dement*. 2024;20:5143-5169.
47. Leuzy A, Mattsson-Carlgren N, Palmqvist S, Janelidze S, Dage JL, Hansson O. Blood-based biomarkers for Alzheimer's disease. *EMBO molecular medicine*. 2022;14:e14408.
48. Liu MN, Lau CI, Lin CP. Precision medicine for frontotemporal dementia. *Frontiers in psychiatry /Frontiers Research Foundation*. 2019;10:75.

49. Cummings J, Lee G, Zhong K, Fonseca J, Taghva K. Alzheimer's disease drug development pipeline: 2021. *Alzheimers Dement (N Y)*. 2021;7:e12179.
50. Cummings J, Zhou Y, Lee G, Zhong K, Fonseca J, Cheng F. Alzheimer's disease drug development pipeline: 2023. *Alzheimers Dement (N Y)*. 2023;9:e12385.
51. Lasagna-Reeves CA, Castillo-Carranza DL, Sengupta U, et al. Identification of oligomers at early stages of tau aggregation in Alzheimer's disease. *FASEB J*. 2012;26:1946-1959.
52. Goedert M, Jakes R, Vanmechelen E. Monoclonal antibody AT8 recognises tau protein phosphorylated at both serine 202 and threonine 205. *Neurosci Lett*. 1995;189:167-169.
53. Malia TJ, Teplyakov A, Ernst R, et al. Epitope mapping and structural basis for the recognition of phosphorylated tau by the anti-tau antibody AT8. *Proteins*. 2016;84:427-434.
54. Porzig R, Singer D, Hoffmann R. Epitope mapping of mAbs AT8 and tau5 directed against hyperphosphorylated regions of the human tau protein. *Biochem Biophys Res Commun*. 2007;358:644-649.
55. Augustinack JC, Schneider A, Mandelkow EM, Hyman BT. Specific tau phosphorylation sites correlate with severity of neuronal cytopathology in Alzheimer's disease. *Acta Neuropathol*. 2002;103:26-35.
56. Braak E, Braak H, Mandelkow EM. A sequence of cytoskeleton changes related to the formation of neurofibrillary tangles and neuropil threads. *Acta Neuropathol*. 1994;87:554-567.
57. Braak H, Thal DR, Ghebremedhin E, Del Tredici K. Stages of the pathologic process in Alzheimer disease: age categories from 1 to 100 years. *J Neuropathol Exp Neurol*. 2011;70:960-969.
58. Koss DJ, Jones G, Cranston A, Gardner H, Kanaan NM, Platt B. Soluble pre-fibrillar tau and beta-amyloid species emerge in early human Alzheimer's disease and track disease progression and cognitive decline. *Acta Neuropathol*. 2016;132:875-895.
59. Lantero-Rodriguez J, Montoliu-Gaya L, Benedet AL, et al. CSF p-tau205: a biomarker of tau pathology in Alzheimer's disease. *Acta Neuropathol*. 2024;147:12.
60. Zhou XW, Li X, Bjorkdahl C, et al. Assessments of the accumulation severities of amyloid beta-protein and hyperphosphorylated tau in the medial temporal cortex of control and Alzheimer's brains. *Neurobiol Dis*. 2006;22:657-668.
61. Sun Y, Guo Y, Feng X, et al. Norovirus P particle-based tau vaccine-generated phosphorylated tau antibodies markedly ameliorate tau pathology and improve behavioral deficits in mouse model of Alzheimer's disease. *Signal transduction and targeted therapy*. 2021;6:61.
62. Tan W, Thiruppathi J, Hong SH, et al. Development of an anti-tauopathy mucosal vaccine specifically targeting pathologic conformers. *NPJ vaccines*. 2024;9:108.
63. Bhaskar K, Konerth M, Kokiko-Cochran O, Cardona A, Ransohoff R, Lamb B. Regulation of tau pathology by the microglial fractalkine receptor. *Neuron*. 2010;68:19-31.
64. Maphis N, Jiang S, Xu G, et al. Selective suppression of the alpha isoform of p38 MAPK rescues late-stage tau pathology. *Alzheimers Res Ther*. 2016;8:54.
65. Hulse J, Bhaskar K. Crosstalk Between the NLRP3 Inflammasome/ASC speck and amyloid protein aggregates drives disease progression in Alzheimer's and Parkinson's disease. *Front Mol Neurosci*. 2022;15:805169.
66. Liu YS, Baxi M, Madan CR, et al. Brain age of rhesus macaques over the lifespan. *Neurobiol Aging*. 2024;139:73-81.

SUPPORTING INFORMATION

Additional supporting information can be found online in the Supporting Information section at the end of this article.

How to cite this article: Maphis N, Hulse J, Peabody J, et al. Targeting of phosphorylated tau at threonine 181 by a Qβ virus-like particle vaccine is safe, highly immunogenic, and reduces disease severity in mice and rhesus macaques. *Alzheimer's Dement*. 2025;21:e70101.
https://doi.org/10.1002/alz.70101